Chemical Geology 479 (2018) 286–301

Contents lists available at ScienceDirect

Chemical Geology

journal homepage: www.elsevier.com/locate/chemgeo

Origin of methane and light hydrocarbons in natural fluid emissions: A key study from Greece

Kyriaki Daskalopoulou[a,b], Sergio Calabrese[a], Fausto Grassa[c], Konstantinos Kyriakopoulos[b], Francesco Parello[a], Franco Tassi[d], Walter D'Alessandro[c,*]

[a] Università degli Studi di Palermo, Dipartimento della Terra e del Mare, via Archirafi, 36, 90123 Palermo, Italy
[b] National and Kapodistrian University of Athens, Department of Geology and Geoenvironment, Panepistimioupolis, Ano Ilissia, 15784 Athens, Greece
[c] Istituto Nazionale di Geofisica e Vulcanologia, via Ugo la Malfa 153, 90146 Palermo, Italy
[d] Università degli Studi di Firenze, Dipartimento della Terra, via G. La Pira 4, 50121 Florence, Italy

ARTICLE INFO

Editor: Dong Hailiang

ABSTRACT

Greece, a country characterised by intense seismic and volcanic activity, has a complex geodynamic and geological setting that favours the occurrence of many gas manifestations. In this study, we address the origin of CH_4 and light hydrocarbons in cold and thermal emissions discharging along the Hellenic territory. Also, we investigate their possible relationship with the main geochemical composition of the gases and the different geological settings of the sampling sites. For this purpose we collected 101 new samples that were analysed for their chemical (O_2, N_2, CH_4, CO_2, He, Ne, Ar, H_2, H_2S and C_2-C_6 hydrocarbons) and isotopic (R/R_A, $\delta^{13}C$-CO_2, $\delta^{13}C$-CH_4 and δ^2H-CH_4) composition. Results show that CH_4 presents a wide range of concentrations (from < 0.5 to 925,200 μmol/mol) and isotopic values ($\delta^{13}C$-CH_4 from −79.8 to +45.0‰ vs. V-PDB; δ^2H-CH_4 from −311 to +301‰ vs. V-SMOW). Greece was subdivided in four geologic units (External [EH] and Internal [IH] Hellenides, Hellenic Hinterland [HH] and active Volcanic Arc [VA]) and a decreasing CH_4 concentration from EH to HH was recognized, whereas CH_4 showed intermediate concentrations in VA. The $CH_4/(C_2H_6 + C_3H_8)$ ratios (from 1.5 to 93,200), coupled with CH_4 isotopic features, suggest that the light alkanes derive from different primary sources and are affected by secondary processes. An almost exclusive biotic, mainly microbial, origin of CH_4 can be attributed to EH gases. Cold gases at IH have mainly a thermogenic origin, although some gases connected to continental serpentinization may have an abiogenic origin. Methane in gases bubbling in thermal waters of IH, HH and VA and fumarolic gases of the VA seem to have an abiogenic origin, although their chemical and isotopic characteristics may have been produced by secondary oxidation of thermogenic CH_4, a process that in some of the sampled gases causes extremely positive isotopic values ($\delta^{13}C$-CH_4 up to +45.0‰ vs. V-PDB and δ^2H-CH_4 up to +301‰ vs. V-SMOW).

1. Introduction

Geogenic emissions of carbon greenhouse gases (mainly CO_2 and CH_4) have a significant impact on the global carbon budget (Kvenvolden, 1993; Klusman and Jakel, 1998; Mörner and Etiope, 2002). Notwithstanding, a reliable estimation of the effective amount discharged from natural manifestations is still a challenge (Guliyev and Feizullayev, 1997; Milkov, 2000 and references therein; Etiope et al., 2009). Methane, the most abundant organic gas compound in Earth's atmosphere, has a potential global warming 28 times higher than that of CO_2 on a 100-year time horizon (Ciais et al., 2013; Etiope, 2015). In a natural environment, the production of CH_4 involves organic matter either as an active (microbial production) or as a passive agent (thermogenic degradation) (Schoell, 1980, 1988; Whiticar, 1999a, 1999b). Microbial activity by Archaea occurring during the diagenesis of sediments at relatively low temperatures (up to 122 °C – Takai et al., 2008) predominantly produces methane, subordinately ethane and, likely, trace amounts of propane (Formolo, 2010). On the other hand, thermogenic methane is produced at higher temperatures (> 150 °C – Quingley and MacKenzie, 1988) by the thermal cracking of organic matter (catagenesis) or oil. Thermogenic gases can be either independent from oil reservoirs or associated with them, having variable amounts of ethane, propane, butane, and condensate (C_{5+} higher hydrocarbons).

Abiogenic processes able to synthesize CH_4 from inorganic molecules at high temperatures, have been also hypothesized to occur in

* Corresponding author.
E-mail address: walter.dalessandro@ingv.it (W. D'Alessandro).

https://doi.org/10.1016/j.chemgeo.2018.01.027
Received 17 August 2017; Received in revised form 19 January 2018; Accepted 23 January 2018
Available online 31 January 2018

natural environments (Etiope and Sherwood Lollar, 2013). Among others, reduction of graphite (Holloway, 1984) or, thermal decomposition of siderite (McCollom, 2013) has been proposed. However, the main abiotic process is considered to be the reduction of gaseous CO or CO_2 (Berndt et al., 1996; Horita and Berndt, 1999; Foustoukos and Seyfried, 2004). The reduction process occurs mainly through the so-called Fischer-Tropsch-type reactions, which are the Fischer-Tropsch reaction (sensu stricto).

$$(2n + 1)\,H_2 + nCO \rightarrow C_nH_{2n+2} + nH_2O \quad (1)$$

that allows also the production of minor amounts of light hydrocarbons and the Sabatier reaction:

$$4H_2 + CO_2 \rightarrow CH_4 + 2\,H_2O \quad (2)$$

Both reactions have high activation energies but in the presence of catalysts, such as native transition metals like Fe, Co, Cr or Ni in natural systems, these reactions occur also in the 100–300 °C range (McCollom, 2013), while recently Etiope and Ionescu (2015) suggested that CH_4 can be effectively produced in the temperature range 20–90 °C in the presence of Ru catalyst within chromite-rich serpentinized rocks.

The Hellenic territory has an intense geodynamic activity, giving rise to (i) the highest seismicity of whole Europe (Burton et al., 2004), (ii) the presence of an active volcanic arc (Pe-Piper and Piper, 2002) and many areas of anomalous high geothermal gradient (Fytikas and Kolios, 1979), and (iii) the widespread occurrence of cold and thermal springs (D'Alessandro and Kyriakopoulos, 2013). As commonly observed in many hydrothermal systems worldwide distributed (e.g., Capaccioni et al., 1993, 2004; Tassi, 2004; Tassi et al., 2005a, 2005b, 2012), the natural fluid discharges in the Hellenic territory contain significant concentrations of CH_4 and light hydrocarbons. Although parts of the Hellenic territory have been target for oil and gas exploration, only limited chemical and isotopic data have been published about these gases (Kamberis et al., 2000; Rigakis et al., 2001; Etiope, 2009; Etiope et al., 2013a). Some data exist also for some hydrothermal systems (Fiebig et al., 2009, 2013, 2015; D'Alessandro et al., 2014) and for gases deriving from on-land serpentinization processes (Etiope et al., 2013; D'Alessandro et al., 2017) for the same area. The present work, through a widespread sampling of gas manifestations, constrains the origin of CH_4 and the postgenetic modifications that could affect the sampled gases all over Greece. To this end, we collected 101 samples from fumarolic, thermal and cold discharges and analysed the concentrations of major (O_2, N_2, CH_4, CO_2) and minor gas species (He, Ne, Ar, H_2, H_2S, C_2H_6, C_3H_8, C_3H_6, *i*-C_4H_{10}, *n*-C_4H_{10} C_3H_6, *i*-C_4H_8 and C_6H_6) as well as the carbon isotopic composition of CH_4 and CO_2, the hydrogen isotopic composition of CH_4 and the isotopic composition of He. These data, integrated by literature data (Rigakis et al., 2001; Etiope, 2009; Etiope et al., 2006; Etiope et al., 2013a; 2013b; D'Alessandro et al., 2014, 2017), were used to relate origin and postgenetic processes affecting CH_4 to the geolithologic situation of the sampled manifestations.

1.1. Study area

The geotectonic evolution of the broader area of Greece has been described as a discontinuous southwestward migration of the Alpine orogenic process with successive subductions of the Tethyan oceanic basins, producing collisional tectonics in the areas between Eurasia and Gondwana during Mesozoic and Tertiary times (Robertson and Dixon, 1984; Mountrakis, 1985, 1986). According to the plate tectonics theory, new palaeogeographic and tectonic models were proposed about the evolution of Tethys and the emplacement of the ophiolites (Dercourt, 1972; Roberts and Koukouvelas, 1996; Bortolotti and Principi, 2005; van Hinsbergen et al., 2005). Based on these models, the Aegean Region was divided into several isopic/structural zones. According to various authors (Smith and Moores, 1974; Mountrakis, 1985, 2010), who described the gradual rifting of various continental fragments of Gondwana at the beginning of the Mesozoic, their independent motion toward Eurasia that created new oceanic crust to the rear, and their final collision with the Eurasia at the end of the Mesozoic, the structural zones (Fig. 1) from west to east can be subdivided, as follows:

a) External Hellenides: i) Parnassos; ii) Gavrovo-Tripolis; iii) Paxos zones that correspond to a neritic continental sea depositional environment; iv) Ionian zone that stands for a neritic intracontinental basin with pelagic sediments; v) Pindos zone that is formed from sedimentary remnants.
b) Internal Hellenides: i) Circum-Rhodope zone that includes volcanoclastic deposits, sea deposits ending up in deep-sea sediments westwards, flysch and molasses; ii) Vardar/Axios zone that is characterised by deep-sea sediments and the obducted ophiolites; iii) Pelagonian zone consisting of neritic sediments; iv) Subpelagonian zone with the obducted ophiolites; v) Attico-Cycladic zone that is envisaged as a continental fragment having undergone neritic sedimentation.
c) Hellenic Hinterland: i) Rhodope and ii) Serbomacedonian Massifs. Both Massifs represent an old continental crust affected by Alpidic metamorphism and consist of Precambrian-Silurian crystalline rocks (Anders et al., 2006; Reischmann and Kostopoulos, 2007) bearing few neritic deposits and also document Late Eocene – Early Oligocene granitoid intrusions (Fig. 1).

To sum up, the Hellenides are the result of the collision of several microcontinental fragments with the margin of Eurasia through the Cretaceous and Paleogene (van Hinsbergen et al., 2005). After the collision, the Hellenides have been characterised by widespread extension, particularly since the Miocene, as a result of subduction rollback from the oceanic crust of the African plate. The modern fault pattern is a result of the westward and south-westward motion of the Aegean-Anatolian microplate with respect to the Eurasian plate.

The Paleogene Hellenide orogeny of Greece and its eastward continuation into western Turkey resulted from the collision of the Apulian microcontinental fragment in the Eocene to Oligocene with the Pelagonian, Rhodope, and Serbo-Macedonian fragments, which had previously accreted to the southern margin of Eurasia in the Cretaceous. Subsequent extension in the Aegean was rapid, likely due to subduction rollback over residual oceanic crust of the African plate, whereas Anatolia had been bounded by African continental crust south of Cyprus since the Early Miocene. This regional extension and the thermal effects of asthenospheric upwelling, related to changes in the geometry of subducting slabs, have been interpreted as causing magma genesis principally within the lithospheric mantle (Pe-Piper and Piper, 2002). Ophiolites were mostly exposed in the Pindos and Vardar oceanic basins, forming two subparallel ophiolitic zones. Their emplacement took place at the closure of the Mesozoic Neotethys, initially in the Upper Jurassic–Lower Cretaceous and finally during the post-Paleocene times (e.g. Ferrière et al., 2016; Papanikolaou, 2009; Robertson, 2004, 2012; Stampfli et al., 2003). At the south Aegean Volcanic Arc, the activity started during the Upper Pliocene (Fytikas et al., 1986) and is currently active. The calc-alkaline volcanic activity of the Southern Aegean region developed in various volcanic centres from Sousaki to Nisyros through Methana, Milos and Santorini.

2. Materials and methods

Names, sampling date and coordinates of all new sampling sites can be found as supplementary material in Table S1. Bubbling gases were sampled using an inverted funnel positioned above the bubbles, whereas soil gases were collected by inserting a pipe in the soil at > 50 cm depth and driving the gas by a syringe and a 3-way valve. Dry gases were collected in 12 mL Exetainer® vials (only for hydrocarbon analyses) and in glass flasks equipped with two stopcocks (for the remaining analyses). Dissolved gas samples were collected by using of

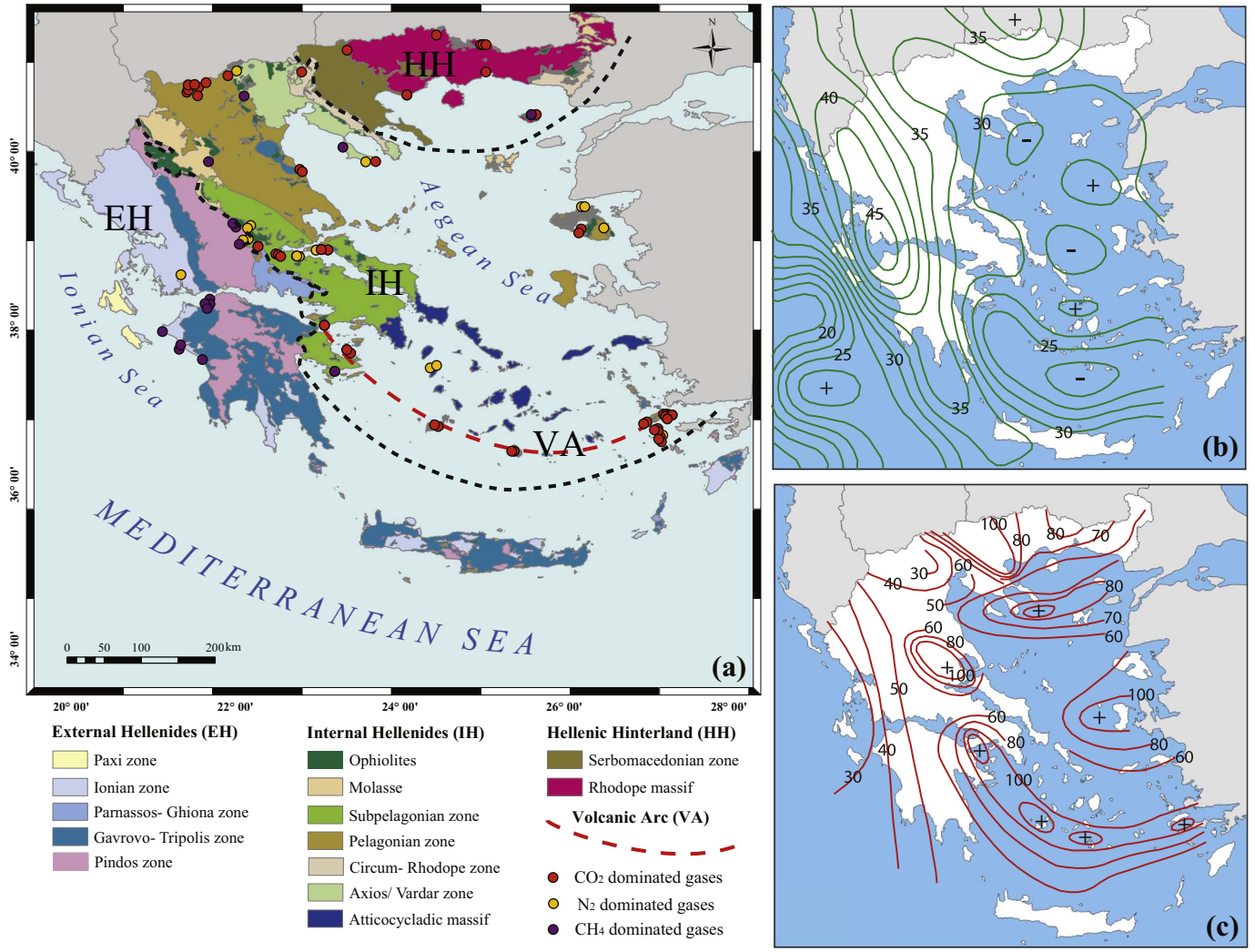

Fig. 1. a) Map of the structural zones of the Hellenides (after Mountrakis, 1986) with the sampling sites of this study. Circles indicate the sampling sites subdivided on the basis of the dominating gas species (violet for CH_4; orange-red for CO_2; yellow-orange for N_2); b) The Moho depth model (km) as proposed by Grigoriadis et al. (2016) and c) Heat flow map (mW/cm^2) as proposed by Fytikas and Kolios (1979). (For interpretation of the references to colour in this figure legend, the reader is referred to the web version of this article.)

glass vials sealed by gas tight rubber/teflon plugs and analysed applying the "*headspace technique*" following the method proposed by (Capasso and Inguaggiato, 1998). To allow rapid comparison, dissolved gases have been recalculated as free gas phase in equilibrium with the sampled water. These, expressed in μmol/mol, have been obtained from the partial pressure values taking into account the solubility coefficients of each gas species at laboratory temperature.

In the laboratory, samples were analysed for He, H_2, H_2S, O_2, N_2, CH_4 and CO_2 by gas-chromatography (Perkin Elmer Clarus500 equipped with a double Carboxen 1000 columns, TCD-FID detectors) using Ar as the gas carrier. Ar was analysed with a Perkin Elmer XL gas-chromatograph with MSieve 5A column, TCD detector having He as carrier. Analytical uncertainties were ± 5%. Hydrocarbon analyses were performed with a Shimadzu 14a gas-chromatograph equipped with a Flame Ionization Detector (FID) using He as the carrier gas (Vaselli et al., 2006). The analytical error was ≤5%.

Carbon isotope composition of CO_2 was determined by using a Thermo Delta Plus XP, coupled with a Thermo TRACE Gas Chromatograph (GC) and a Thermo GC/C III interface. The TRACE GC is equipped with a Poraplot Q (25 m × 0.32 mm) column and uses Helium (5.6) as carrier gas at a constant flow of 0.9 cm^3 min^{-1}. Undesired gas species, such as N_2, O_2, and CH_4, are vented to atmosphere by means of back-flush of He and a Sige valve.

The $^{13}C/^{12}C$ ratios are reported as $\delta^{13}C_{CO2}$ values with respect to the V-PDB standard. Carbon isotope ratios were determined by comparing three in-house standards ($\delta^{13}C$ ranging from +0.3 ± 0.1‰ to −28.5 ± 0.3‰ vs V-PDB calibrated by using of a CO_2 standard (RM8564) with known isotopic composition ($\delta^{13}C = -10.45 \pm 0.04$‰ vs V-PDB) and two international standards (NBS 18 and NBS 19). External precision, computed as1σ (standard deviation) on ten measurements of the same sample, is 0.1‰.

Carbon and Hydrogen isotopes of CH_4 both in free gases and in dissolved gases were measured using a Thermo TRACE GC interfaced to a Delta Plus XP gas source mass spectrometer and equipped with a Thermo GC/C III (for Carbon) and with GC/TC peripherals (for Hydrogen).

The gas chromatograph was equipped with an Rt-Q Plot column (Restek 30 m × 0.32 mm i.d.) and the oven was held at a constant temperature (50 °C for carbon and 40 °C for Hydrogen). The flow rate of carrier gas (He of 5.6 grade) was held at a constant flux of 0.8 cm^3 min^{-1}. A split/splitless injector with a split ratio from 10:1 to 80:1 was used for sample introduction, except for diluted samples (CH_4 concentration lower than 10 mmol/mol) when direct on-column injection was performed.

The inlet system, better described in Grassa et al. (2010), consists of a stainless steel loop with a known volume (50 μl), connected to a two-position six-port Valco® valve. Before the introduction of the sample, a vacuum of 10^{-2} mbar measured with an EBRO pressure gauge is

ensured by a rotary vane pump. Once CH_4 was separated from the gas mixture, it was quantitatively converted to CO_2 by passing through a combustion oven (T = 940 °C) for $^{13}C/^{12}C$ ratios analysis or to H_2 by passing it through a reactor set at a temperature of 1440 °C for $^{2}H/^{1}H$ ratios analysis. Each sample analysis took about 500 s.

The $^{13}C/^{12}C$ ratios are reported as $\delta^{13}C$-CH_4 values with respect to the V-PDB standard and $^{2}H/^{1}H$ ratios are reported here as $\delta^{2}H$-CH_4 values with respect to the V-SMOW standard. Carbon isotope ratios were determined by comparing an in-house standard ($\delta^{13}C = -49.5 \pm 0.2‰$) calibrated by using of four CH_4 standards (Isometric Instruments) with known isotopic composition ($\delta^{13}C$ ranging from $-23.9 \pm 0.3‰$ to $-66.5 \pm 0.3‰$ vs V-PDB).

Hydrogen isotope ratios were determined comparing an in-house standard ($\delta^{13}C = -200 \pm 2.0‰$) with a CH_4 standard with known isotopic composition ($\delta^{2}H = -186.1 \pm 3.0‰$ vs V-SMOW).

External reproducibility, estimated as 1σ (standard deviation) on ten measurements of the same sample, is 0.2‰ and 2.0‰ for carbon and hydrogen isotopes respectively.

In CO_2-dominated gases having CH_4 concentrations lower than 1000 μmol/mol, the analyses of the isotope ratios of methane were carried out in the headspace gas samples collected using pre-evacuated 60 mL glass flasks filled with 20 mL of a 4 N NaOH solution (Giggenbach and Gougel, 1989).

The abundance and isotope composition of He, and the $^{4}He/^{20}Ne$ ratios, were determined by separately admitting He and Ne into a split flight tube mass spectrometer (Helix SFT). Helium isotope compositions are given as R/R_A, where R is the ($^{3}He/^{4}He$) ratio of the sample and R_A is the atmospheric ($^{3}He/^{4}He$) ratio ($R_A = 1.386 \times 10^{-6}$). The analytical technique is described more in detail in Paonita et al. (2012). The analytical errors were generally < 1%.

3. Results

3.1. Chemical composition of the gases

On the basis of the spatial distribution of the gas discharges and their type of emission, the whole dataset was subdivided into 4 main geological domains, as follows: 1) External Hellenides (EH) - 17 samples; 2) Internal Hellenides (IH) - 60 samples; 3) Hellenic Hinterland (HH) - 8 samples; 4) Volcanic Arc (VA) - 33 samples. The chemical composition of the dry gas fraction (CO_2, H_2S, CH_4, N_2, O_2, Ar, He and H_2) of the 101 gas samples analysed in the present study is reported in Table 1, whereas the 17 literature data were taken from Rigakis et al., 2001, Etiope, 2009, Etiope et al., 2006; Etiope et al., 2013a, 2013b, D'Alessandro et al., 2014, 2017. Dry gases were dominated by either CO_2 (from 18 to 997,000 μmol/mol) or N_2 (from 1100 to 989,000 μmol/mol) or CH_4 (from < 0.5 to 913,000 μmol/mol) gas species (Fig. 2a). O_2 and Ar showed concentrations up to 177,000 and 12,000 μmol/mol respectively. H_2S was either below detection limit or showing concentrations generally lower than 10,000 μmol/mol except for the fumaroles of Nisyros, where the concentrations reached up to 192,000 μmol/mol (Fiebig et al., 2013). He concentrations were up to 2240 μmol/mol.

In the CO_2-CH_4-N_2 ternary diagram samples collected in the EH show CH_4 (thermal emissions) and CH_4-N_2 dominated gases (cold emissions) with relative low contents of CO_2 (25–34,000 μmol/mol). Gases collected from the thermal manifestations of the IH are rich in N_2-CO_2, whereas in the remaining cold manifestations the CO_2-rich gases are prevailing although sometimes they showed relatively high concentrations of N_2 (samples 8, 17, 18, 28, 29, 89 and 90). In this area, three CH_4-dominated gases (samples 1, 50 and 82, with 880,000, 764,000 and 576,000 μmol/mol respectively) were also found. In HH, CO_2 is the most abundant gas species, except for samples 78 and 79 that have dominant N_2 (537,000 and 417,000 μmol/mol respectively). The thermal emissions of the VA are CO_2-dominated, except sample 86 that is showing relatively high N_2 (368,000 μmol/mol). Most gases collected from the cold emissions of the same region show the same chemical features as the gases discharged from the thermal springs, with the exception of samples 67, 73, 74, 87 and 102 that were N_2-dominated.

The He-N_2-Ar ternary diagram (Giggenbach, 1996) (Fig. 2b) suggests important mixing processes between deep crustal or mantle gases and also gases originating in the upper crust or atmosphere. The N_2/Ar ratio can be used to distinguish the relative contributions to a gas mixture from air, air-saturated waters, and fluids deriving from interactions within subducting and crustal rocks/sediments and mantle gases (e.g. Snyder et al., 2001, 2003). CH_4-N_2 rich gases of the EH and some of the CO_2 dominated cold emissions of the IH plot close to the Air and Air Saturated Water (ASW) points, indicating a dominant atmospheric component for these gases. Some of the samples from VA and the cold emissions of IH (CO_2 dominated) fall on the theoretical line that connects ASW with a He-rich source with a relatively low contribution of crustal N_2 (Giggenbach, 1996). Samples of the HH rich in CO_2 and some of the emissions that occur in the IH, characterised by a N_2-CO_2 composition, show atmospheric N_2 mixed with non-atmospheric He.

3.2. Isotope composition of the gases

The $\delta^{13}C$-CO_2 values ranged from −20.1 to +8.5‰ although most of them are comprised in a narrower isotopic range from −7.5 to +0.5‰ (Table 2). Samples from EH have negative values, from −14.1 to −7‰. The $\delta^{13}C$-CO_2 values of the gases collected from IH, are in a wide range (from −16‰ to +8.5‰). In HH, they show a narrower range (−2.4 to +0.3‰), whereas in VA they range from −3.5 to 0.4‰, apart from the sample 67 whose $\delta^{13}C$-CO_2 value was −20.1‰. Gases collected from emissions of IH and HH, in which N_2-CO_2 are the dominant species, show a range of values of $\delta^{13}C$-CO_2 that vary between −16 to −0.9‰ and −1.9 to 0.3‰, respectively.

CO_2 dominated gases from VA show relatively high values for the isotopic ratio of He (from 0.21 to 6.71 R/R_A; Table 2), whereas cold and thermal gases that occur in HH and IH are characterised by values that reach up to 0.41 and 1.27 R/R_A, respectively (Table 2). The N_2-CH_4 dominated gas samples from EH show values from 0.08 to 0.41 R/R_A, whereas the N_2-rich cold manifestations from IH show values in the range of 0.3–0.97 R/R_A.

3.3. Hydrocarbons

3.3.1. Chemical composition of the hydrocarbons

Gases from EH show the highest concentrations of CH_4, having a median of 721,200 μmol/mol (from 85,000 to 925,000 μmol/mol). In IH, they present a median of 2600 μmol/mol with values ranging from < 0.5 up to 880,000 μmol/mol, whereas the lowest concentrations are found in HH with a median of 545 μmol/mol (from 23 up to 879 μmol/mol). Finally, those collected in VA present a median of 1460 μmol/mol (from 5 up to 117,000 μmol/mol).

3.3.2. Isotopic composition of CH_4

The $\delta^{13}C$ and $\delta^{2}H$ values of CH_4 range from −79.8 to +45.0‰ for $\delta^{13}C$-CH_4 and from −311 to +301‰ for $\delta^{2}H$-CH_4, respectively (Table 2). Gases from EH have $\delta^{13}C$-CH_4 and $\delta^{2}H$-CH_4 values ranging from −79.8 to −31.3‰ and from −248 to −62‰, respectively. In IH, the values of $\delta^{13}C$ range from −64 up to +45‰, whereas $\delta^{2}H$ shows a wide range of values (from-311 to +301‰). The $\delta^{13}C$-CH_4 vales of the HH gases range from −34 up to +1‰, whereas their $\delta^{2}H$ values, apart from sample 75 (−174‰), were not measured due to the too low concentrations. The gases from VA show $\delta^{13}C$-CH_4 values ranging from −38 up to +2‰ and $\delta^{2}H$ values from −135 to +36‰.

Table 1
Chemical composition of the gases.

N.	Sample	He	H_2	O_2	N_2	CH_4	CO_2	H_2S	Ar
		μmol/mol	μmol/mol	μmol/mol	μmol/mol	μmol/mol	μmol/mol	μmol/mol	μmol/mol
1	Katakali	4.0	11	589	82,500	880,000	25,000	< 5	1640
2	Psoroneria	887	< 0.5	100	427,000	1120	573,000	< 10	3940
3	Psoroneria	487	< 2	1700	336,000	631	658,000	< 5	3900
4	Thermopyles	322	< 2	59	218,000	1010	760,000	< 5	1980
5	Thermopyles	240	< 2	709	176,000	859	831,000	< 5	1910
6	Koniavitis	581	< 5	50	701,000	2090	281,000	2200	8340
7	Kammena Vourla	700	3.5	100	644,000	3360	352,000	< 10	6050
8	Kammena Vourla	727	< 5	218	588,000	4070	402,000	< 5	5940
9	Kallydica	325	< 2	161,000	508,000	1090	332,000	< 5	n.d.
10	Gialtra	112	< 5	137,000	765,000	302	44,000	n.d.	n.d.
11	Thermopotamos	0.4	< 5	1200	2800	27	977,000	48	40
12	Thermopotamos	1.5	< 2	4700	18,400	1200	958,500	< 5	275
13	Patra	1.7	50	301	192,000	704,000	11,100	< 5	3500
14	Sousaki well	1.3	10	1700	7500	33	975,000	2500	95
15	Sousaki cave	33.0	< 5	4100	37,400	10,100	937,000	511	279
16	Ilion	100	< 5	940	78,900	1820	899,000	< 5	733
17	Ilion	100	3.7	1100	79,400	1800	901,000	< 5	742
18	Ilion sea	199	< 2	11,300	271,000	1040	694,000	< 5	5030
19	Pausanias	< 5	< 5	2300	12,900	53	983,000	< 5	222
20	Pausanias sea	< 5	< 5	6100	14,500	32	984,000	< 5	214
21	Thiafi sea	22.0	< 2	34,100	103,000	916	832,000	< 5	n.d.
22	Agia paraskevi sea	3.1	21.0	10,600	27,000	470	964,000	< 5	458
23	Agia paraskevi sea 2	92.0	100	3900	40,500	11,000	946,000	3100	555
24	Xyna	91.0	1.6	13,000	49,600	215	943,000	< 5	815
25	PPG-1	0.4	< 2	50	40,100	913,000	21,400	< 5	1180
26	Soulanta	31.0	22	125	350,000	649,000	25	n.d.	n.d.
27	Smokovo	100	27	272	124,000	850,000	25	n.d.	n.d.
28	Ekkara	4.0	16	177,000	750,000	5720	25	n.d.	n.d.
29	Ekkara creek	21.0	11	2500	888,000	77,700	552	< 5	10,200
30	Ypati	14.0	0.6	104	42,400	4460	934,000	1260	742
31	Loutra Ypatis	105	< 2	14,500	76,300	5810	888,000	385	848
32	Leonidas	275	< 2	9200	242,000	799	726,000	< 5	2600
33	Kokkinonero	1.6	< 5	2500	7200	249	955,000	n.d.	195
34	Kokkinonero 2	209	< 5	4300	382,000	867	581,000	n.d.	5040
35	Edipsos stadium	< 4	< 2	525	3000	689	967,000	< 5	57
36	Ag. Paraskevi	4.3	< 5	158	23,500	521	929,000	17,400	502
37	Giatsovo soil	12.5	2.0	760	20,800	2690	987,000	< 5	622
38	Analipsi	19.2	< 2	4600	29,600	2350	952,000	< 5	128
39	Tropeouchos	29.0	< 5	76	20,000	6200	952,000	n.d.	233
40	Mesochori gas	4.0	1.5	1000	6500	479	985,000	< 5	42
41	Mesochori 3	1.1	< 5	50	2100	214	975,000	< 5	29
42	Synergio	0.4	< 5	187	1100	< 0.5	997,000	< 5	24
43	Sarri	0.3	< 5	93	1400	95	983,000	n.d.	62
44	Itea	36.0	1.4	5700	38,300	2600	951,000	< 5	223
45	Pozar	474	< 5	56,200	617,000	< 1	323,000	< 5	7660
46	Promachoi	223	< 5	54,400	827,000	2.0	108,000	n.d.	9090
47	Loutrochori 2	374	< 5	175	510,000	436,000	32,400	< 5	6290
48	Xino Nero (Kilkis)	< 5	< 5	2900	15,200	23	965,000	< 5	304
49	Xino Nero 2 (Kilkis)	6.0	< 5	7300	26,000	82	939,000	< 5	n.d.
50	Sani	762	12	330	226,000	764,000	1500	< 5	870
51	Thermopigi	15.0	< 5	639	13,300	669	967,000	< 5	218
52	Eleftheres	31.0	< 2	690	72,600	703	921,000	< 5	1180
53	Polychnitos	192	< 5	3200	193,000	32,800	766,000	< 5	4690
54	Lisvori	471	< 5	5200	519,000	20,500	444,000	< 5	7300
55	Eftalou	1370	< 5	14,400	948,000	219	27,200	< 5	10,400
56	Skala Sikaminias	1280	134	1400	657,000	70,500	259,000	< 5	10,800
57	Kolpos Geras	1020	< 5	16,100	922,000	10	41,200	< 5	9780
58	Milos Skinopi	63.0	< 5	16,700	73,700	4630	829,000	n.d.	n.d.
59	Milos DEH	8.0	< 5	2200	9600	818	978,000	n.d.	n.d.
60	Kefalos	18.0	27	3290	25,100	23,900	946,000	< 5	105
61	Kos Paradise	14.0	< 2	3100	8600	12,100	959,000	< 5	170
62	Kos Kokkinonero	5.0	3.1	3200	13,600	2970	978,000	< 5	171
63	KKN1	3.3	295	3500	24,400	2400	980,000	673	n.d.
64	Kos Kokkinonero 2	4.3	30	2700	8300	3140	991,000	< 5	n.d.
65	KVO2	34.0	1980	10,100	75,400	21,000	877,000	54	n.d.
66	KVO52	44.0	2.9	317	4000	23,100	947,000	851	31
67	Ag. Irini 2	446	< 2	2210	989,000	6240	900	< 5	7520
68	Ag. Irini 1	0.9	< 2	3900	9200	24	963,000	15	200
69	Gyali nord	0.5	3.7	2600	9600	5.0	966,000	< 5	266
70	Gyali	9.0	< 2	2200	23,300	68	956,000	< 5	354
71	Gyali lake	21.0	< 2	716	139,000	525	869,000	3800	n.d.
72	Gyali west	5.0	31	1570	8300	21,000	970,000	< 5	71

(*continued on next page*)

Table 1 (*continued*)

N.	Sample	He	H_2	O_2	N_2	CH_4	CO_2	H_2S	Ar
		μmol/mol	μmol/mol	μmol/mol	μmol/mol	μmol/mol	μmol/mol	μmol/mol	μmol/mol
73	Katsouni	120	< 2	11,500	855,000	134	155,400	< 5	11,500
74	Lies	135	< 2	18,800	643,000	140	315,200	< 5	9790
75	Nea Kessani	26.0	< 2	5900	14,700	386	987,000	< 5	208
76	Eleftheres Ag. Marina	51.0	< 2	3400	180,000	756	809,300	< 5	2760
77	Paranesti 2	< 5	< 5	1700	8700	102	963,200	< 5	n.d.
78	Thermes (Xanthi)	2240	< 5	9700	537,000	844	467,000	< 5	8090
79	Thermes 3 (Xanthi)	1570	< 5	588	417,000	879	573,900	< 5	7350
80	Thermia (Kos)	2.4	< 5	1100	8900	51	994,600	< 5	211
81	Thermia sea (Kos)	16.0	< 2	2500	42,400	278	955,000	< 5	98
82	Therma Limani	0.10	15	53	7900	576,000	363,000	< 5	150
83	Geotrisi	128	97	1200	30,200	94,900	857,000	< 5	624
84	Ag. Anargyroi Kithnos	1100	< 2	2800	664,000	833	329,000	< 5	8420
85	Kolona	726	< 2	26,800	836,000	0.90	136,000	< 5	8400
86	Nea Kameni	6.0	8100	83,600	367,000	264	526,000	< 5	4740
87	Erinia (N. Kameni)	245	< 2	42,800	651,000	1300	301,000	< 5	9510
88	Ag. Anargyroi	< 5	48	14,700	957,000	27,000	1360	n.d.	n.d.
89	Ag. Anargyroi 2	< 5	17	18,200	779,000	203,000	250	n.d.	n.d.
90	Archani	12.9	< 10	7420	948,000	44,700	18	n.d.	n.d.
91	Lysimachia	9.9	< 10	978	602,000	363,000	34,800	n.d.	n.d.
92	Kaitsa	123	< 10	3070	655,000	316,000	26,200	300	n.d.
93	Amplas	83.4	27	1780	199,000	800,000	29	n.d.	n.d.
94	Platystomo	345	< 10	907	860,000	128,000	10,700	n.d.	n.d.
95	PP9S Nisyros	16.0	14,800	100	2500	2520	779,000	173,000	n.d.
96	S4 Nisyros	20.0	8240	581	6500	7510	822,000	151,000	n.d.
97	A13 Nisyros	21.0	9540	100	1390	1460	813,000	175,000	n.d.
98	S15 Nisyros	19.0	8050	700	21,900	4350	769,000	192,000	n.d.
99	K7 Nisyros	10.0	6670	695	6300	32,400	891,000	47,600	n.d.
100	Thermia (Kos)	2.5	< 2	535	9300	64	989,000	< 5	98
101	Ag. Irini 2	412	< 2	2000	613,000	117,000	256,000	< 5	n.d.

n.d. = not determined.

4. Discussion

4.1. Origin of the inorganic gases

Nitrogen, one of the main components found in the gas samples, shows generally decreasing concentrations from the EH and IH to the HH (Fig. 3a). Gases from the VA display on average even lower contents (Fig. 3a). As previously seen in the He-N_2-Ar ternary diagram (Fig. 2b), it mostly originates from the atmosphere through the meteoric recharge or through diffusion in the shallowest soil layers. From the same diagram a contribution from crustal sources or from the subducting slab is apparent. At the moment only few N-isotopic values of N_2 have been published (Grassa et al., 2010) confirming significant (about 60%) sedimentary contribution.

In Fig. 4a it is noticeable that most of the CO_2-rich cold manifestations from IH plot close to the atmospheric point suggesting an important atmospheric contribution for He. Gases from EH present in their majority a crustal origin for He whereas those from VA indicate a strong mantle contribution. Most N_2-CO_2 dominated gases from IH seem to be fed by a mixed mantle-crustal source with a mantle component

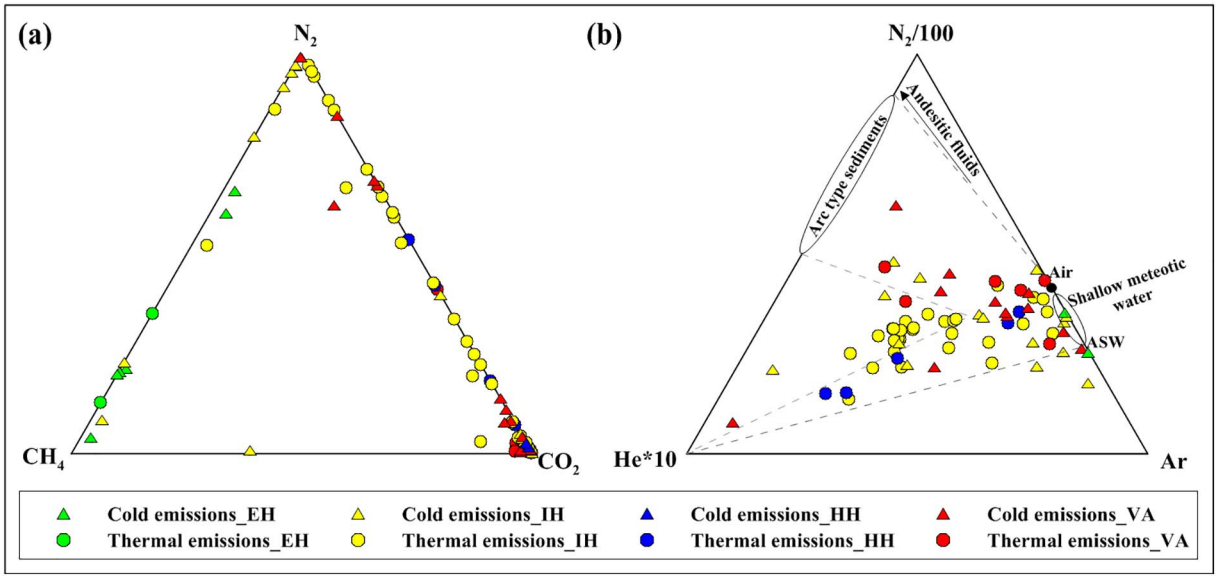

Fig. 2. Chemical composition of the collected gases. (a) CH_4-N_2-CO_2 ternary diagram and (b) He-N_2-Ar ternary diagram. Symbol colours refer to the geographical distribution of the samples, while shape refers to the type of the emission (cold or thermal).

Table 2
Isotopic composition of the gases.

N.	$\delta^{13}C(CO_2)$	$\delta^{13}C(CH_4)$	$\delta^{2}H(CH_4)$	R/R_A	$^4He/^{20}Ne$
	‰	‰	‰		
1	8.5	−64.3	−216	n.d.	n.d.
2	n.d.	−2.3	129	0.07	281
3	−5.4	10.9	301	0.07	95.1
4	−5.3	1.4	30	0.20	228
5	−5.3	−4.2	79	0.20	208
6	−9.8	−10.6	n.d.	n.d.	n.d.
7	−7.4	6.3	62	0.53	159
8	−7.5	4.6	60	0.51	106
9	−13.3	5.3	n.d.	n.d.	n.d.
10	n.d.	n.d.	n.d.	0.46	23.8
11	−3.1	−21.4	−115	0.43	8.5
12	−2.7	−21.7	−124	0.44	3.2
13	−14.1	−79.8	−211	0.39	0.59
14	−1.2	−20.9	−117	0.46	8.6
15	−1.8	−21.3	−114	0.21	76.7
16	−2.6	−1.4	57	0.26	5.4
17	−2.5	3.2	32	0.25	252
18	−2.6	45.0	n.d.	n.d.	n.d.
19	−2.9	n.d.	n.d.	n.d.	n.d.
20	n.d.	n.d.	n.d.	n.d.	n.d.
21	−3.4	−38.6	n.d.	n.d.	n.d.
22	−2.0	−5.6	−49	0.79	0.61
23	−2.2	−5.0	−68	0.74	308
24	−2.5	n.d.	n.d.	n.d.	n.d.
25	−7.0	−74.5	−210	0.41	0.77
26	n.d.	−60.8	−248	0.07	7.8
27	n.d.	−44.9	−196	0.04	44.0
28	n.d.	−33.8	−276	0.34	2.0
29	n.d.	−33.5	−234	0.30	1.0
30	−3.2	−38.7	n.d.	0.13	6.3
31	−4.4	−32.9	−105	0.05	122
32	−6.0	n.d.	n.d.	n.d.	n.d.
33	−0.8	−19.8	−37	0.23	2.3
34	n.d.	n.d.	n.d.	n.d.	n.d.
35	−3.0	n.d.	n.d.	n.d.	n.d.
36	−6.7	−3.8	n.d.	0.74	5.9
37	−0.6	−25.7	−151	0.47	189
38	−0.7	−23.4	−145	0.23	29.8
39	−1.2	−29.4	−187	n.d.	n.d.
40	−1.3	−21.0	−131	0.62	5.1
41	−0.4	−22.5	n.d.	0.66	50.7
42	−0.8	n.d.	n.d.	0.57	1.4
43	n.d.	n.d.	n.d.	0.56	1.6
44	0.5	−27.7	−157	0.30	15.3
45	−5.4	n.d.	n.d.	0.82	44.5
46	−7.2	n.d.	n.d.	1.27	30.3
47	−16.0	−18.8	−113	n.d.	n.d.
48	−2.4	1.1	n.d.	0.26	14.8
49	n.d.	n.d.	n.d.	n.d.	n.d.
50	−9.4	−57.0	−180	0.68	1490
51	−2.1	−1.1	n.d.	0.65	107
52	−1.1	−23.5	n.d.	0.41	36.5
53	−2.0	−19.9	−106	0.82	82.2
54	−3.9	−7.2	−21	0.85	97.0
55	−11.8	n.d.	n.d.	0.83	103
56	−4.5	−24.8	n.d.	0.92	183
57	−9.0	n.d.	n.d.	0.43	67.1
58	−2.1	−8.1	−29	n.d.	n.d.
59	n.d.	n.d.	n.d.	n.d.	n.d.
60	−0.6	−12.3	−54	6.21	92.8
61	−0.1	−19.5	−136	6.49	224
62	−1.9	−18.3	n.d.	2.38	12.8
63	−1.0	−18.2	n.d.	n.d.	n.d.
64	n.d.	n.d.	n.d.	n.d.	n.d.
65	0.3	−13.4	n.d.	n.d.	n.d.
66	−0.5	−18.0	−128	6.71	1070
67	−20.1	−12.5	−14	3.88	48.3
68	−2.5	n.d.	n.d.	0.85	5.9
69	−0.7	n.d.	n.d.	4.22	1.6
70	−1.2	n.d.	n.d.	4.98	25.8
71	−2.1	n.d.	n.d.	n.d.	n.d.
72	0.4	−16.1	−101	4.62	139
73	−2.7	n.d.	n.d.	3.22	8.7
74	−2.1	n.d.	n.d.	3.35	19.5
75	0.3	−34.8	−174	n.d.	n.d.
76	−1.0	n.d.	n.d.	n.d.	n.d.
77	n.d.	n.d.	n.d.	n.d.	n.d.
78	−1.9	−26.1	n.d.	0.40	335
79	−1.9	−26.3	n.d.	n.d.	n.d.
80	−3.1	n.d.	n.d.	1.04	2.9
81	−3.0	n.d.	n.d.	1.55	44.1
82	6.0	−44.6	−263	0.72	0.74
83	−0.9	−27.7	−143	1.15	185
84	−5.8	34.7	n.d.	0.44	18.1
85	−12.3	n.d.	n.d.	0.51	96.4
86	0.3	n.d.	n.d.	2.65	0.92
87	−2.3	−12.0	n.d.	n.d.	n.d.
88	n.d.	−2.0	−127	0.97	0.82
89	n.d.	−26.6	−301	0.87	0.93
90	n.d.	−35.0	−288	0.38	0.84
91	n.d.	−72.3	−174	n.d.	n.d.
92	n.d.	−49.2	−62	0.08	8.7
93	n.d.	−37.5	−204	0.07	16.4
94	n.d.	−42.3	−154	0.06	17.1
95	−1.7	−22.0	−108	5.66	536
96	−1.6	−23.6	−125	6.08	30.1
97	−2.7	−23.3	−121	5.78	242
98	−2.1	−23.6	−110	5.53	6.8
99	−2.1	−23.3	−130	5.91	29.1
100	−3.5	2.4	36	1.44	40.6
101	−0.8	−16.1	−75	3.67	81.5

n.d. = not determined.

comprised between 1 and 15%. Also gases from HH show a mix between a low mantle component (2–5%) and a prevailing crustal source.

In the $CO_2/^3He$ vs. $\delta^{13}C$-CO_2 binary diagram (Fig. 4b), the CO_2- and N_2-dominated gases from VA and the N_2-CO_2 thermal emissions from IH mostly plot along the mixing line between the mantle and the limestone end-members, showing a low contribution from sedimentary organic-rich sources. The N_2-dominated gases of the cold manifestations from IH show $CO_2/^3He$ ratios even lower than that of mantle gases, which are probably caused by relative CO_2 loss due to its higher solubility in aquatic environments with respect to He (Fig. 4b). This process may explain the extremely low $\delta^{13}C$-CO_2 and $CO_2/^3He$ values shown by sample 67 from the VA (−20.1‰ and 3.7×10^5, respectively), which was characterised by a relatively low concentration of CO_2. Carbon dioxide loss may also be produced by calcite deposition at relatively high pH (Stefánsson et al., 2016, 2017). This process involves deprotonation of CO_2 (aq) to HCO_3^- and CO_3^{-2} and formation of calcite, resulting in a decrease of the $\delta^{13}C$ values of the residual CO_2. It should be noted that most thermal water samples are oversaturated in carbonate minerals and travertine depositions were recognized at some thermal areas (Kanellopoulos, 2012; Winkel et al., 2013; Kanellopoulos et al., 2017).

Hydrogen sulfide in fumarolic gases from active volcanoes is likely produced by thermochemical reduction of magmatic SO_2 occurring within the hydrothermal reservoirs (Giggenbach, 1987) and, therefore, shows the highest concentrations along the VA (Fig. 3f) where most of the geothermal systems evidence an input of magmatic gases (Marini and Fiebig, 2005; Rizzo et al., 2015). Sedimentary sources of H_2S consist of i) alteration of sulfide minerals (Giggenbach, 1980; Chiodini, 1994), ii) microbial activity, and iii) thermochemical sulfate reduction (Machel et al., 1995; Worden and Smalley, 1996). The H_2S concentrations in the gas discharges of EH and HH are below detection limit with few exceptions, likely because this compound has a relatively high solubility in water and/or the lack of significant sources of S-bearing volatile compounds in the regions. Thus, whichever its origin, it may be

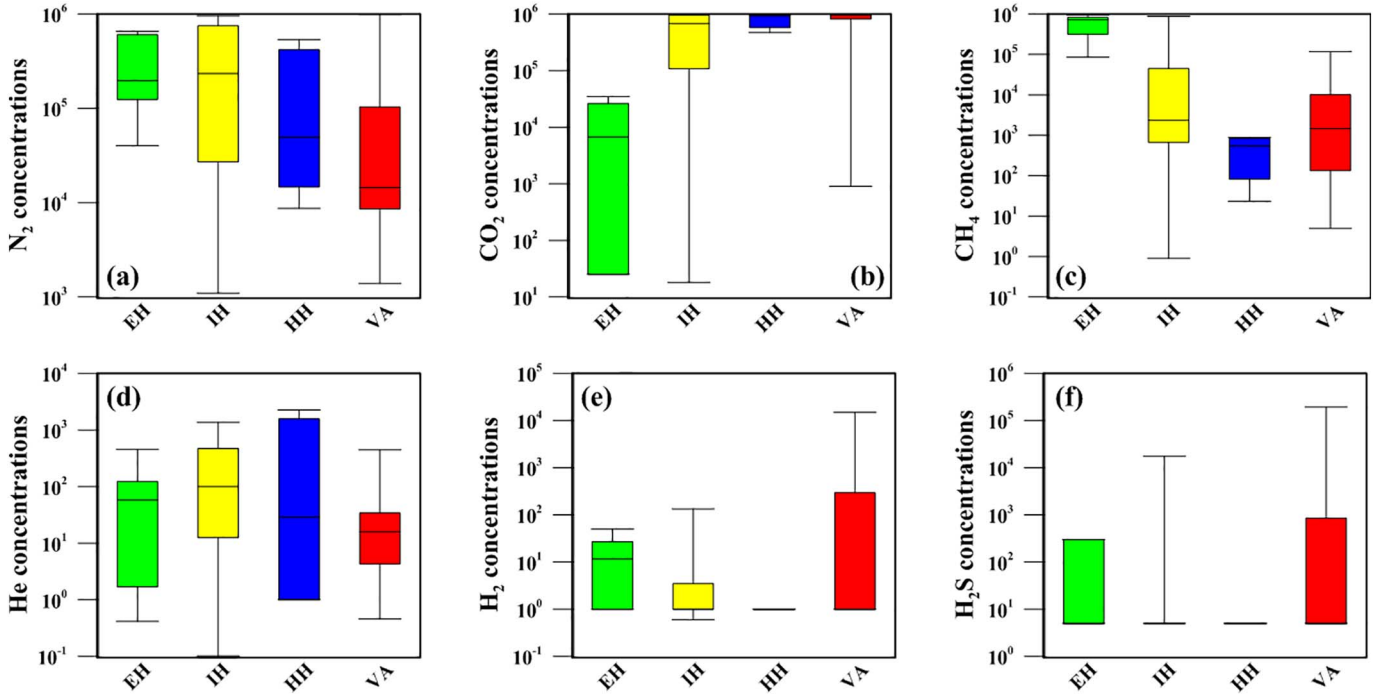

Fig. 3. Box and whiskers plot in which the total range of concentrations (in μmol/mol) of a) N_2; b) CO_2; c) CH_4; d) He; e) H_2 and f) H_2S are presented for each region.

partially or totally dissolved and oxidized in cold shallow aquifers present along the uprising gas pathways (Minissale, 2004). Most gases from IH show also H_2S concentrations below detection limit, excepting samples 6, 23, 30, 31 and 36 where concentrations up to 17,400 μmol/mol have been measured. It is worth noting that these samples were collected in two areas (Sperchios basin and Kassandra peninsula) corresponding to maxima on the heat flow map (Fig. 1c), suggesting the occurrence of medium enthalpy geothermal systems (Fytikas and Kolios, 1979).

The occurrence of relatively high concentrations of H_2 (up to 14,800 μmol/mol; Table 1, Fig. 3e) in gases from the volcanic systems of Nisyros and Santorini is most likely related to water-rock interactions at elevated temperatures. It is well known that Fe(II)-bearing minerals react with water at temperatures > 300 °C generating H_2 (e.g., Giggenbach, 1987; Seewald, 2001). Most of the samples collected at IH and HH have H_2 below detection limit (Table 1). Concentrations of H_2 up to 50 μmol/mol, a gas often linked to hydrocarbon generation, are found in the EH gases related to hydrocarbon reservoirs of the area.

4.2. An overview in the classification of hydrocarbons

Taran and Giggenbach (2003) highlighted that for the description of hydrothermal hydrocarbon production two main mechanisms can be hypothesized. The first one deals with the biotic origin of methane, whereas the second one with its abiotic origin.

Gunter (1978), based on numerous observations, proposed that the nature and distribution of hydrocarbon species in hydrothermal vapours is more consistent with the thermal degradation of kerogen rather than inorganic production, a conclusion also supported by other researchers (e.g., Welhan, 1988; Darling, 1998; Mango, 2000; Taran and Giggenbach, 2003). More specifically, as indicated by Hunt (1996), biotic methane is produced either by microbial or thermogenic processes.

The second approach has to do with the formation of abiotic (or

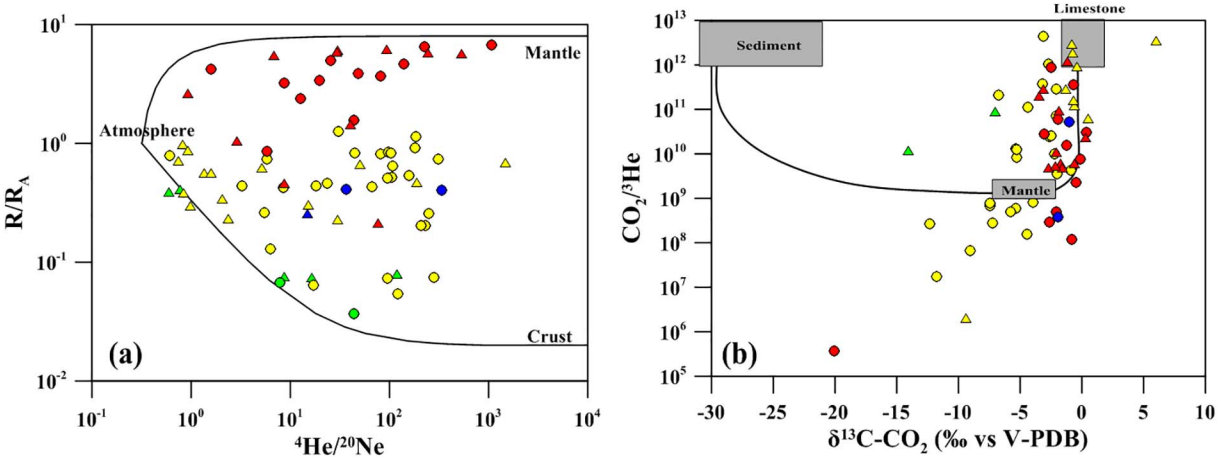

Fig. 4. a) Binary plot of R/R_A vs. $^4He/^{20}Ne$ of the Hellenic gas emissions. The mixing lines between Atmosphere and Mantle and between Atmosphere and Crust are also plotted, b) Binary plot of $CO_2/^3He$ vs. $\delta^{13}C(CO_2)$ The composition for Sediments, MORB-like Mantle and Limestones end-members are, as follows: $\delta^{13}C(CO_2) = -30‰$, $-5‰$ and 0‰ and $CO_2/^3He = 1 \times 10^{13}$, 2×10^9 and 1×10^{13}, respectively (Sano and Marty, 1995). Symbols as in Fig. 3.

abiogenic) methane by chemical reactions that do not require the presence of organic matter. These reactions include magmatic processes and gas-water-rock reactions (for example Fischer Tropsch type reactions (Fischer and Tropsch, 1923, 1926)) occurring over a wide range of temperatures (Etiope and Sherwood Lollar, 2013). These processes refer to the formation of organic compounds from a gaseous mixture of CO and H_2 in high temperature and pressure surface-catalysed process, involving sequential reduction and polymerization of single-carbon units (McCollom and Seewald, 2007; McCollom, 2013; Konn et al., 2015), (see Reaction (1)). From this process, it is noticeable that trace amounts of abiotic hydrocarbons can occur in volcanic and geothermal fluids. Moreover, considerable amounts of methane, reaching concentrations of 80–90 vol%, have also been discovered in an increasing number of sites in Precambrian crystalline shields, in serpentinized ultramafic rocks along mid-ocean ridges and in land-based ophiolites, peridotite massifs, and igneous intrusions (Etiope and Sherwood Lollar, 2013).

Considering these mechanisms, generally, although not exclusively, the origin of CH_4 can be investigated using the classification diagrams proposed by Bernard and Schoell (Bernard et al., 1978; Schoell, 1980, 1988; Etiope and Schoell, 2014, Fig. 6a, b). Bernard et al. (1978) introduced correlation between $CH_4/(C_2H_6 + C_3H_8)$ concentration ratios and the δ^{13}C-CH_4 ratios to qualitatively distinguish CH_4 derived from microbial and thermogenic sources. Furthermore, other researchers (Whiticar et al., 1986; Schoell, 1988; Burke et al., 1988, 1988; Whiticar, 1999a, 1999b; Hornibrook et al., 1997; Chanton et al., 2005) hypothesized that the production of CH_4 is associated with inverse or antipathetic shifts in δ^2H and δ^{13}C of CH_4, in which fermentation of acetate will result in CH_4 enriched in ^{13}C and depleted in ^{2}H, something relative to CH_4 produced via the CO_2 reduction pathway. In those diagrams (Fig. 6a, b), thermogenic CH_4 has been reported to exhibit δ^{13}C-CH_4 values ranging from −50 to −30‰ and δ^2H-CH_4 values ≤150‰ (e.g., Schoell, 1980; Whiticar, 1999a, 1999b; Bradley and Summons, 2010). Microbial CH_4 usually has δ^{13}C-CH_4 values ≤50‰ (e.g. Whiticar, 1999a, 1999b; McCollom and Seewald, 2007) and can be produced either by i) methyl-type fermentation or by ii) carbonate reduction (^{13}C-depleted and ^{2}H-enriched CH_4 with respect to the methyl-type fermentation) (Whiticar et al., 1986; Whiticar, 1999a, 1999b). CO_2-reduction and acetate fermentation pathways may be distinguished also on the basis of the carbon isotope fractionation factor (α_C) between coexisting CO_2 and CH_4 (Whiticar et al., 1986).

$$\alpha_C = (\delta^{13}C - CO_2 + 1000)/(\delta^{13}C - CH_4 + 1000) \quad (3)$$

The isotope fractionation of the carbon dioxide reduction is generally between $\alpha_C = 1.055$ and 1.09, in contrast to acetate- type fermentation which is usually between $\alpha_C = 1.04$ and 1.055.

Gases produced by the decay of organic matter at $T > 150$ °C (thermogenic gases) are commonly characterised by $CH_4/(C_2H_6 + C_3H_8)$ concentration ratios (known as the "Bernard parameter") < 100, with the exception of coal gases (Whiticar, 1999a, 1999b) and shale gases (Tilley and Muehlenbachs, 2013). Higher ratios (> 1000) are expected when hydrocarbon production derives exclusively from microbial activity (Whiticar and Suess, 1990; Jenden et al., 1993). However, many processes can play a fundamental role for its origin, such as isotopic fractionation by diffusion (Prinzhofer and Battani, 2003), secondary methanogenesis and anaerobic biodegradation (Dimitrakopoulos and Muehlenbachs, 1987; Pallasser, 2000; Etiope et al., 2009). Methanotrophic bacteria, for instance, may oxidize biogenic CH_4, causing a shift toward less negative isotopic values of the residual gas (Coleman et al., 1981).

CH_4 of abiogenic origin, e.g. discharged from high-temperature hydrothermal fluids venting from sediment-free ultramafic systems, is thought to be characterised by δ^2H-CH_4 values higher than −150‰ (Welhan and Craig, 1983; Proskurowski et al., 2006, 2008; McCollom and Seewald, 2007; Bradley and Summons, 2010). Similarly, the δ^{13}C-CH_4 values of CH_4 produced from water-rock reactions, such as hydration of ultramafic rocks, may vary in a wide range because it depends on the inorganic carbon source and the magnitude of carbon isotope fractionation.

Another possible source of abiogenic CH_4 is the serpentinization process of ultramafic rocks within ophiolitic sequences. Such processes produce significant quantities of H_2 even at temperatures below 100 °C (Miller et al., 2017) mainly through the following reactions:

$$\underset{\text{olivine}}{2(Mg,Fe)_2SiO_4} + 3H_2O \rightarrow \underset{\text{serpentine}}{(Mg,Fe)_3Si_2O_5(OH)_4} + \underset{\text{brucite}}{(Mg,Fe)(OH)_2} \quad (4)$$

$$\underset{\text{serpentine (greenalite)}}{Fe_3Si_2O_5(OH)_4} + H_2O \rightarrow \underset{\text{magnetite}}{Fe_3O_4} + \underset{\text{silica}}{2SiO_2} + H_2 \quad (5)$$

The produced H_2 in turn may be transformed in CH_4 reacting with carbon oxides (CO, CO_2 or simple organic acids). Such reactions can be mediated either microbially or inorganically (Fischer-Tropsch type reactions – Etiope and Sherwood Lollar, 2013). The latter are favoured at high temperatures but experiments show that they can proceed even at ambient temperature in the presence of a suitable catalyst (Etiope and Ionescu, 2015). Apart from significant H_2 and CH_4 gas production, the serpentinization processes lead to the formation of hyperalkline groundwaters (Barnes and O'Neil, 1969; Bruni et al., 2002).

Besides few exceptions (Hinrichs et al., 2006), Bernard and Schoell diagrams (Bernard et al., 1978; Schoell, 1980, 1988; Etiope and Schoell, 2014, Fig. 6a, b) work fairly well for the classification of CH_4 from thermogenic and microbial sources, however they are of limited use considering the identification of abiogenic CH_4. The reason is that there seems to be a considerable overlap of fields characteristic for thermogenic CH_4, thermogenic CH_4 affected by secondary oxidation and "abiogenic" CH_4. Furthermore, some studies evidenced that in carbon limited conditions the Carbon isotopic composition of CH_4 deriving from microbial activity could reach values as high as those generally attributed to abiogenic origin (Kietäväinen and Purmako, 2015).

Recently, new proxies such as clumped isotopes, capable of determining the isotopologues of CH_4 molecules (Stolper et al., 2014; Wang et al., 2015), have been developed. Potential applications of this method include determination of CH_4 formation temperature (CH_4 thermometry), and detection of kinetic isotope fractionation, both of which might be used in separating biotic from abiotic CH_4 (Stolper et al., 2014; Wang et al., 2015). More applications are expected when this method comes more widely attainable.

4.3. Origin of hydrocarbon compounds in Greece

Taking into consideration the geo-lithological division of the study areas and the dominant gas species, it is noticeable that the manifestations found on the western part of Greece display higher CH_4 concentrations (Fig. 3c) with respect to those found in the eastern part where CO_2 is the prevailing gas species (Figs. 1a, 2a and 3b). In particular, EH are characterised by widespread and thick sedimentary formations mainly originating from the erosion of elder rocks from IH and HH. This geological/petrological regime makes the stratigraphic sequences of EH richer in solid organic substances, as also supported by the hydrocarbon deposits occurring in this area (Palacas et al., 1986). On the other hand, IH and HH are characterised by more "mature" formations (Cavazza et al., 2014), mainly intrusive and metamorphic, and by significant erosion causing a substantial reduction of the crustal thickness before the post-orogenic extension. These formations contain much less organic matter than EH. Therefore, as also seen in Fig. 6a and b, the occurrence of biogenic CH_4 in these areas is likely related to the presence of a post-orogenic sedimentary cover.

The most used parameters to discriminate the genetic processes of CH_4 are the C- and H-isotopic compositions of CH_4 (Schoell, 1980; Etiope and Schoell, 2014) and the $CH_4/(C_2H_6 + C_3H_8)$ ratio (Bernard et al., 1978). Of course, it should be considered that secondary

Table 3
Concentrations of C_2-C_6 hydrocarbons.

N.	C_2H_6	C_3H_8	C_3H_6	i-C_4H_{10}	n-C_4H_{10}	i-C_4H_8	i-C_5H_{12}	n-C_5H_{12}	C_6H_6	$CH_4/(C_2H_6 + C_3H_8)$
	μmol/mol	μmol/mol	μmol/mol	μmol/mol	μmol/mol	μmol/mol	μmol/mol	μmol/mol	μmol/mol	
1	112	2.8	b.d.l.	0.12	b.d.l.	b.d.l.	b.d.l.	b.d.l.	b.d.l.	7667
2	21	3.7	0.018	2.3	2.1	3.7	0.45	0.45	4.9	45
3	15	3.6	0.02	1.8	2.1	2.6	0.42	0.51	5.6	34
4	13	2.8	0.03	2.6	1.2	1.5	0.55	0.33	2.2	64
5	11	2.2	0.04	2.1	1.5	1.4	0.48	0.25	1.8	65
6	5.1	1.3	b.d.l.	0.45	1.1	0.68	0.33	0.21	0.56	327
7	8.7	2.2	b.d.l.	0.85	0.71	1.3	0.36	0.31	0.66	308
8	13	3.6	0.01	1.4	1.7	1.5	0.62	0.33	0.98	245
9	3.1	0.85	b.d.l.	0.33	0.75	0.55	0.69	0.25	0.44	276
10	1.1	0.08	b.d.l.	b.d.l.	b.d.l.	0.51	b.d.l.	b.d.l.	0.54	256
11	1.1	0.29	b.d.l.	0.12	0.17	0.22	0.09	0.05	0.28	19
12	8.6	2.3	0.03	0.62	1.3	0.95	0.26	0.39	5.4	110
13	95	11	b.d.l.	b.d.l.	b.d.l.	b.d.l.	b.d.l.	b.d.l.	b.d.l.	6645
14	n.d.	n.d.	n.d.	n.d.	n.d.	n.d.	n.d.	n.d.	n.d.	n.c.
15	2.1	b.d.l.	b.d.l.	b.d.l.	b.d.l.	b.d.l.	b.d.l.	b.d.l.	b.d.l.	4810
16	15	3.1	0.06	2.5	3.1	5.5	1.3	0.66	5.1	101
17	13	3.3	0.08	2.3	2.6	4.4	1.5	0.71	4.5	110
18	3.8	0.46	b.d.l.	0.15	0.16	0.11	0.08	0.06	0.71	244
19	2.3	0.51	b.d.l.	0.15	0.26	0.75	0.08	0.11	0.85	19
20	1.5	0.23	b.d.l.	0.11	0.22	0.54	0.05	0.08	0.77	18
21	10	2.1	0.02	1.1	0.65	0.85	0.44	0.26	0.77	76
22	6.1	1.5	0.02	1.1	0.66	0.74	0.21	0.22	1.2	62
23	1.5	0.11	b.d.l.	b.d.l.	0.06	b.d.l.	b.d.l.	b.d.l.	b.d.l.	6832
24	3.4	0.56	0.02	0.41	0.36	0.41	0.56	0.15	0.74	54
25	123	3.5	b.d.l.	0.15	b.d.l.	b.d.l.	b.d.l.	b.d.l.	b.d.l.	7221
26	2960	278	0.21	126	178	155	26	35	215	201
27	321	8.5	b.d.l.	b.d.l.	b.d.l.	b.d.l.	b.d.l.	b.d.l.	b.d.l.	2579
28	11	3.3	b.d.l.	1.2	1.3	1.6	0.56	0.61	0.98	400
29	13	0.51	b.d.l.	b.d.l.	b.d.l.	b.d.l.	b.d.l.	b.d.l.	b.d.l.	5751
30	13	3.1	b.d.l.	2.5	1.4	1.5	0.39	0.33	0.91	277
31	6.5	0.85	b.d.l.	0.41	0.85	0.76	0.05	0.13	1.4	790
32	4.3	0.85	0.02	0.41	0.69	0.64	0.15	0.22	2.1	155
33	2.4	0.39	b.d.l.	0.15	0.21	0.26	0.05	0.06	0.65	89
34	2.1	0.33	b.d.l.	0.11	0.25	0.29	0.11	0.12	0.58	357
35	6.6	1.3	0.04	0.55	1.1	0.88	0.12	0.26	3.7	87
36	6.7	1.6	b.d.l.	0.55	0.69	1.3	0.25	0.36	2.4	63
37	12	2.5	0.04	1.5	2.1	3.6	1.1	0.66	1.8	186
38	15	2.9	0.03	1.1	2.6	3.1	0.74	0.51	2.2	131
39	3.1	0.15	b.d.l.	b.d.l.	b.d.l.	b.d.l.	b.d.l.	b.d.l.	b.d.l.	1908
40	7.7	2.1	0.03	1.2	0.77	1.1	0.25	0.26	1.5	49
41	8.9	1.8	0.006	1.1	0.85	1.3	0.21	0.21	1.7	20
42	b.d.l.	b.d.l.	b.d.l.	b.d.l.	b.d.l.	b.d.l.	b.d.l.	b.d.l.	b.d.l.	n.c.
43	b.d.l.	b.d.l.	b.d.l.	b.d.l.	b.d.l.	b.d.l.	b.d.l.	b.d.l.	b.d.l.	n.c.
44	19	3.9	0.11	2.4	2.8	4.9	1.8	0.75	4.1	114
45	b.d.l.	b.d.l.	b.d.l.	b.d.l.	b.d.l.	b.d.l.	b.d.l.	b.d.l.	b.d.l.	n.c.
46	0.08	b.d.l.	b.d.l.	b.d.l.	b.d.l.	b.d.l.	b.d.l.	b.d.l.	b.d.l.	25
47	61	3.9	b.d.l.	b.d.l.	b.d.l.	b.d.l.	b.d.l.	b.d.l.	b.d.l.	6712
48	3.6	0.66	b.d.l.	0.65	0.78	1.2	0.15	0.24	1.8	5.4
49	4.3	0.71	b.d.l.	0.78	0.85	1.6	0.21	0.26	1.9	16
50	85	3.1	b.d.l.	b.d.l.	b.d.l.	b.d.l.	b.d.l.	b.d.l.	b.d.l.	8675
51	5.3	1.3	0.008	0.31	0.39	0.75	0.08	0.07	0.56	101
52	2.3	0.15	0.02	0.11	0.14	0.25	0.08	0.06	0.58	287
53	3.6	b.d.l.	b.d.l.	b.d.l.	b.d.l.	b.d.l.	b.d.l.	b.d.l.	b.d.l.	9111
54	2.3	b.d.l.	b.d.l.	b.d.l.	b.d.l.	b.d.l.	b.d.l.	b.d.l.	b.d.l.	8913
55	12	3.3	0.02	1.4	2.1	3.3	0.55	1.2	2.3	14
56	b.d.l.	b.d.l.	b.d.l.	b.d.l.	b.d.l.	b.d.l.	b.d.l.	b.d.l.	b.d.l.	n.c.
57	0.51	0.18	b.d.l.	0.05	b.d.l.	0.11	b.d.l.	b.d.l.	0.34	14
58	22	5.6	0.008	2.2	2.9	3.7	1.1	1.2	7.1	168
59	9.5	2.1	0.007	1.3	1.1	1.9	0.26	0.31	2.6	71
60	12	0.89	b.d.l.	b.d.l.	b.d.l.	b.d.l.	b.d.l.	b.d.l.	b.d.l.	1853
61	1.6	0.15	b.d.l.	b.d.l.	0.12	b.d.l.	b.d.l.	b.d.l.	0.08	6914
62	7.3	0.33	b.d.l.	0.11	0.21	0.25	0.08	0.05	0.15	389
63	0.15	b.d.l.	b.d.l.	b.d.l.	b.d.l.	b.d.l.	b.d.l.	b.d.l.	b.d.l.	16,000
64	8.1	0.48	b.d.l.	0.16	0.25	0.33	0.12	0.11	0.21	366
65	4.2	0.26	b.d.l.	0.13	0.21	0.25	0.05	b.d.l.	0.11	4709
66	4.3	0.85	b.d.l.	0.54	0.15	0.65	0.15	0.22	1.3	4485
67	7.5	1.2	0.04	0.58	0.74	0.65	0.06	0.11	1.2	718
68	0.45	0.13	b.d.l.	b.d.l.	b.d.l.	0.15	b.d.l.	b.d.l.	0.23	41
69	b.d.l.	b.d.l.	b.d.l.	b.d.l.	b.d.l.	b.d.l.	b.d.l.	b.d.l.	b.d.l.	n.c.
70	0.99	0.23	b.d.l.	0.08	0.11	0.05	b.d.l.	b.d.l.	0.39	56
71	5.1	1.8	0.02	1.7	0.56	0.75	0.35	0.15	1.4	76
72	11	0.33	b.d.l.	b.d.l.	b.d.l.	b.d.l.	b.d.l.	b.d.l.	b.d.l.	1854

(*continued on next page*)

Table 3 (*continued*)

N.	C_2H_6	C_3H_8	C_3H_6	*i*-C_4H_{10}	*n*-C_4H_{10}	*i*-C_4H_8	*i*-C_5H_{12}	*n*-C_5H_{12}	C_6H_6	$CH_4/(C_2H_6 + C_3H_8)$
	μmol/mol	μmol/mol	μmol/mol	μmol/mol	μmol/mol	μmol/mol	μmol/mol	μmol/mol	μmol/mol	
73	3.3	0.59	0.02	0.24	0.25	0.33	0.21	0.15	0.47	34
74	7.6	2.5	0.08	1.1	0.95	1.6	0.78	1.1	2.9	14
75	11	3.9	0.03	1.3	1.5	2.8	0.43	1.1	2.5	26
76	4.6	0.91	0.08	0.45	0.45	0.69	0.11	0.25	2.6	137
77	11	3.3	0.009	1.6	1.9	2.2	0.58	0.91	4.4	7.1
78	6.2	1.5	0.008	1.6	1.8	2.3	0.66	0.91	2.1	110
79	7.6	1.8	0.009	1.5	2	2.6	1.2	1.1	2.5	94
80	4.3	1.1	0.006	0.23	0.36	0.81	0.11	0.13	1.9	9.4
81	3.3	0.65	0.01	0.15	0.33	0.77	0.15	0.19	2.2	70
82	60	3.9	b.d.l.	b.d.l.	b.d.l.	b.d.l.	b.d.l.	b.d.l.	b.d.l.	9013
83	13	0.26	b.d.l.	b.d.l.	b.d.l.	b.d.l.	b.d.l.	b.d.l.	b.d.l.	7157
84	7.8	3.1	0.05	0.56	0.71	0.56	0.54	0.23	1.4	76
85	b.d.l.	b.d.l.	b.d.l.	b.d.l.	b.d.l.	b.d.l.	b.d.l.	b.d.l.	b.d.l.	n.c.
86	5.6	1.1	0.15	0.26	0.54	0.78	0.31	0.11	2.3	39
87	10	1.9	0.06	1.6	1.3	1.1	0.36	0.25	1.4	109
88	n.d.	n.d.	n.d.	n.d.	n.d.	n.d.	n.d.	n.d.	n.d.	n.c.
89	16.8	b.d.l.	b.d.l.	b.d.l.	b.d.l.	b.d.l.	b.d.l.	b.d.l.	b.d.l.	12,072
90	n.d.	n.d.	n.d.	n.d.	n.d.	n.d.	n.d.	n.d.	n.d.	n.c.
91	3.3	0.59	0.02	0.24	0.25	0.33	0.21	0.15	0.47	93,213
92	120	b.d.l.	b.d.l.	b.d.l.	b.d.l.	b.d.l.	b.d.l.	b.d.l.	b.d.l.	2630
93	n.d.	n.d.	n.d.	n.d.	n.d.	n.d.	n.d.	n.d.	n.d.	n.c.
94	n.d.	n.d.	n.d.	n.d.	n.d.	n.d.	n.d.	n.d.	n.d.	n.c.
95	0.9	0.18	b.d.l.	b.d.l.	b.d.l.	b.d.l.	b.d.l.	b.d.l.	b.d.l.	2331
96	n.d.	n.d.	n.d.	n.d.	n.d.	n.d.	n.d.	n.d.	n.d.	n.c.
97	5.51	1.1	b.d.l.	b.d.l.	b.d.l.	b.d.l.	b.d.l.	b.d.l.	b.d.l.	220
98	4.48	0.75	b.d.l.	b.d.l.	b.d.l.	b.d.l.	b.d.l.	b.d.l.	b.d.l.	831
99	n.d.	n.d.	n.d.	n.d.	n.d.	n.d.	n.d.	n.d.	n.d.	n.c.
100	n.d.	n.d.	n.d.	n.d.	n.d.	n.d.	n.d.	n.d.	n.d.	n.c.
101	23	b.d.l.	b.d.l.	b.d.l.	b.d.l.	b.d.l.	b.d.l.	b.d.l.	b.d.l.	5078

b.d.l. = below detection limit; n.d. = not determined; n.c. = not calculated.

processes (e.g. mixing, inorganic or microbially-driven oxidation) affecting CH_4 and light hydrocarbons might change the chemical and isotopic composition of these compounds masking, at least partially, their primary origin (Coleman et al., 1981; Kiyosu and Imaizumi, 1996; Kinnaman et al., 2007). High $CH_4/(C_2H_6 + C_3H_8)$ concentration ratios (> 1000) are generally limited to the "microbial" samples of EH and to many samples from IH, as well as for some samples of VA (Gyali and Kos islands) (Fig. 6a, Table 3). For the remaining samples, the ratio shows lower values, indicating either a preferential loss of CH_4 due to microbial oxidation or the production of significant quantities of low-molecular-weight hydrocarbons through thermal degradation of organic matter. More specifically, in both Bernard and modified Schoell diagrams (Fig. 6a, b), the CH_4-dominated gases from EH plot in the biogenic fields. In particular, samples of the Gavrovo-Tripolis zone have a clear microbial origin with low $\delta^{13}C$ but relatively high δ^2H values of CH_4 that point to a microbial carbonate reduction, whereas those from the Ionian zone seem to be of thermogenic origin (Fig. 6a, b). Some gas samples from the Ionian and of Pindos zones (EH) are intermediate between the thermogenic and microbially-derived group, (Fig. 6b). Such mixing pattern is also confirmed by the $CH_4/(C_2H_6 + C_3H_8)$ ratio measured in gases collected in petroleum exploration wells of the Katakolo hydrocarbon field (NW Peloponnesus), which decreases from pure microbial-type values (1000–12,500) at shallower levels down to low values (3.27–24.4) at deeper levels (2000–2500 m depth) where temperatures for thermogenic gas generation are reached (Kamberis et al., 2000).

Samples ascribable to a microbial origin on the basis of their $\delta^{13}C$ and δ^2H values of CH_4 display α_C values (Fig. 5a) compatible with the CO_2-reduction origin at least for the samples in which both $\delta^{13}C$-CO_2 and $\delta^{13}C$-CH_4 are available (samples 1, 13,25, 50 and 82).

Furthermore, some of the N_2-CO_2 dominated samples collected from the thermal emissions that occur in the Subpelagonian and Vardar/Axios zones (IH) plot in the field characteristic for abiogenic hydrocarbons emitted from volcanic-geothermal systems after McCollom and Seewald (2007) (Fig. 6a). At the same time, also the CO_2-rich thermal manifestations from HH (Rhodope massif) and IH (Pelagonian and Subpelagonian zones) are found in a another field proposed by Sherwood Lollar et al. (2006) to be characteristic for an abiogenic origin, releasing gases mainly related to hydrothermal systems within the crystalline or metamorphic rocks of the Precambrian shield (Anders et al., 2006; Reischmann and Kostopoulos, 2007) (Fig. 6a). In both cases, a contribution from a biogenic source cannot be excluded due to the closeness to the thermogenic field. In the latter case however, the samples are found in low to medium enthalpy back-arc geothermal fields in an area characterised by extensional tectonics, which presumably also results in crust thinning (Fytikas and Kolios, 1979). CO_2 dominated thermal gases from the VA show chemical and isotopic characteristics that are apparently consistent with an abiogenic origin for CH_4 ($\delta^{13}C$-CH_4 values around −20‰, and δ^2H-CH_4 values around −150‰) deriving from CO_2 reduction. Contributions from a biogenic source cannot be excluded for those samples having $CH_4/(C_2H_6 + C_3H_8)$ ratios < 1000 (Bernard ratio ranges from 9 to 4810).

Some N_2-rich gases from IH discharge in correspondence of the ophiolitic bodies that crop out in the Hellenic territory (Pe-Piper and Piper, 2002), where hyperalkaline waters (pH from 9.72 to 11.98) were found at Othrys (central Greece - Etiope et al., 2013b; D'Alessandro et al., 2014) and at Argolida (D'Alessandro et al., 2017). CH_4 collected in these hyperalkaline springs show $\delta^{13}C$-CH_4 values ranging from −37.4 to −26.6‰ and δ^2H-CH_4 from −311 to −250‰, excluding sample 88 that has more positive values (−2.0 and −127‰ respectively) that were attributed by D'Alessandro et al. (2017) to microbial oxidation processes. Such values, on the diagram of Fig. 6b, fall all, except sample 88, within the field of land-based serpentinization systems as defined by Etiope and Schoell (2014) and have been attributed by the previous authors to an abiogenic origin (Etiope et al., 2013b; D'Alessandro et al., 2014, 2017).

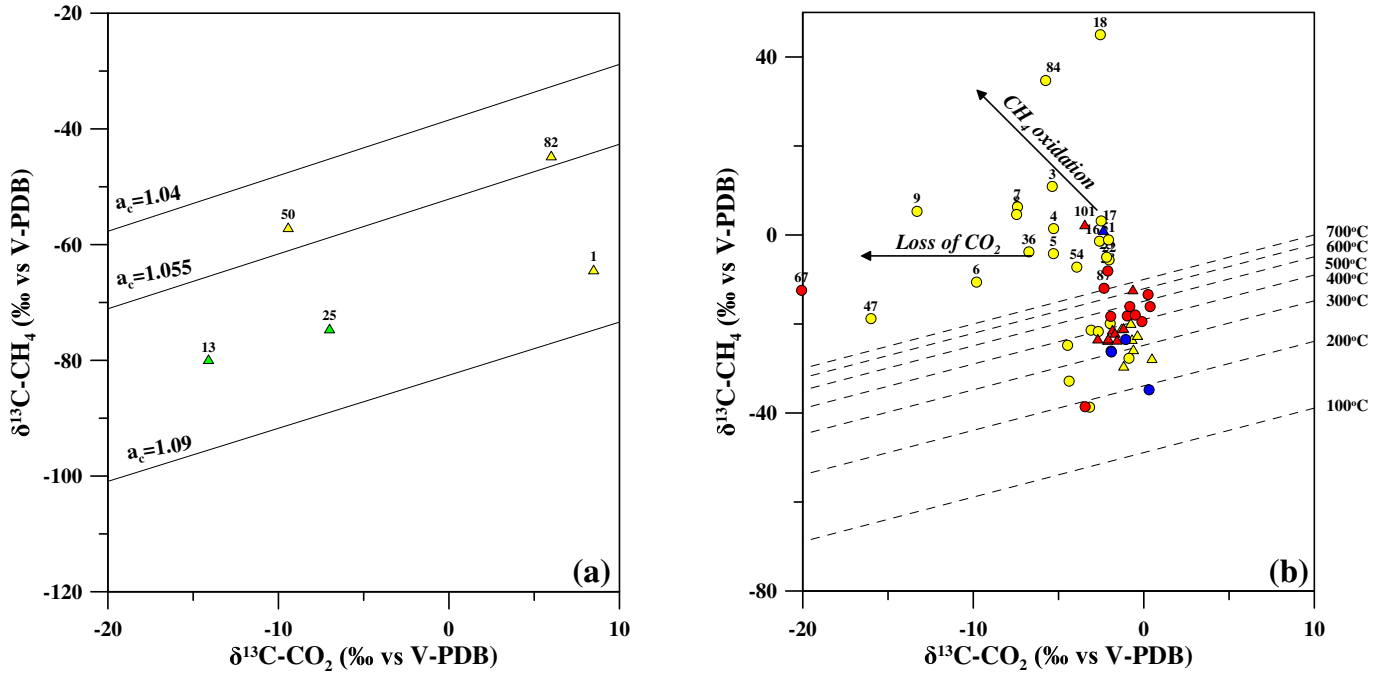

Fig. 5. a) $\delta^{13}C–CO_2$ vs. $\delta^{13}C–CH_4$. Carbon isotope fractionation factor (α_C) is based on the Whiticar et al. (1986) functions, b) $\delta^{13}C–CO_2$ vs. $\delta^{13}C–CH_4$. Temperature scales are based on the isotope fractionation factors from Bottinga (1969).

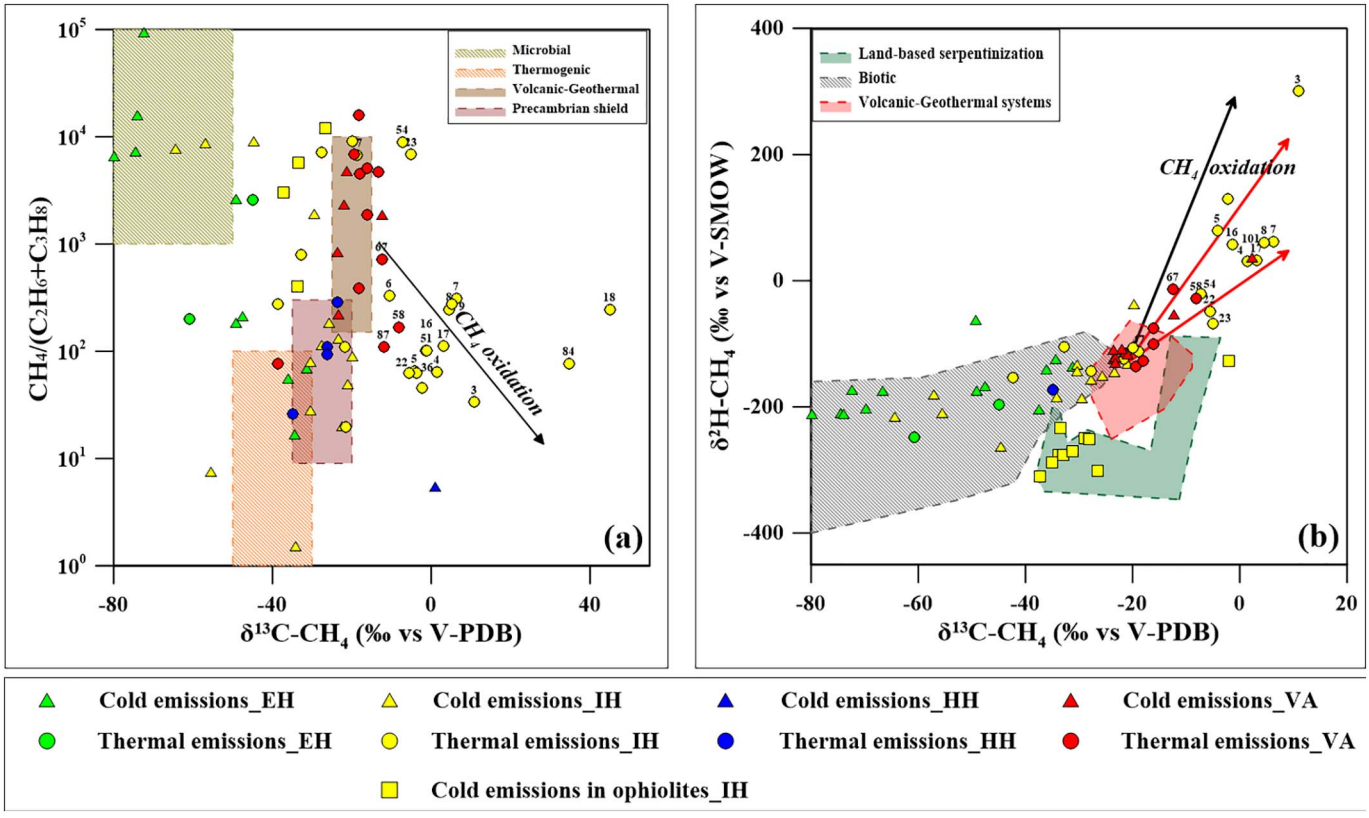

Fig. 6. a) Bernard diagram (Bernard et al., 1978) correlating the $CH_4/(C_2H_6 + C_3H_8)$ concentration ratios with the $\delta^{13}C$-CH_4 isotopic composition of the Hellenic gas discharges. Values for gases of biogenic origin (microbial and thermogenic) and for Precambrian Shield and Geothermal fields are reported (McCollom and Seewald, 2007, and references therein) for comparison, b) modified Schoell binary diagram (Etiope and Schoell, 2014) between δ^2H-CH_4 and $\delta^{13}C$-CH_4 ratios for the Hellenic gas discharges. Slopes of biogenic and abiogenic oxidation of CH_4 are respectively plotted as red- and black-coloured lines. (For interpretation of the references to colour in this figure legend, the reader is referred to the web version of this article.)

4.4. Secondary post-genetic processes

Many processes can significantly modify the isotopic signature of primary methane. Methanotrophic bacteria, for instance, may oxidize biogenic CH_4, causing a shift toward less negative isotopic values of the residual gas (Coleman et al., 1981).

The majority of the thermal gases of Subpelagonian and Vardar/Axios zones (IH), the cold manifestations of the Rhodope massif (HH) and some of the volcanic-hydrothermal ones show low $CH_4/[C_2H_6 + C_3H_8]$ ratios (Fig. 6a, Table 3) and strongly positive isotopic ratios of CH_4 ($\delta^{13}C$ up to +45‰ and δ^2H up to +301‰ – Fig. 6a, b, Table 2). Such chemical and isotopic features were likely caused by oxidation of CH_4 (Fig. 5b). In these environments, microbes obtain energy from aerobic or anaerobic CH_4 oxidation (Murrell and Jetten, 2009), preferentially consuming CH_4 with respect to higher hydrocarbons and preferring light isotopes. Thermophilic and acidophilic methanotrophs oxidize CH_4 also in the harsh environment of thermal waters up to temperatures of more than 80 °C (Sharp et al., 2014). The temperatures of the sampling sites in which we found enriched $\delta^{13}C$ and δ^2H values for CH_4 are mostly in the range from 40 to 63 °C but reaching up to 73.7 °C in the case of sample 54. Although until now, no microbiological studies have been made on these waters to definitely support the occurrence of methanotrophs, the measured temperatures are well within the range that allows the presence of methane oxidizing microorganisms.

Inorganic oxidation of CH_4 (Kiyosu and Imaizumi, 1996) in some samples cannot be ruled out. Nevertheless, the isotopic fractionations of organic and inorganic oxidation of CH_4 follow different fractionation paths. The former follows $\Delta H/\Delta C$ slopes ranging from 5.9 to 13 (Cadieux et al., 2016 and references therein) and the latter a slope of 21 (Kiyosu and Imaizumi, 1996). Since in our samples it is not always possible to establish the primary isotopic composition before oxidation, we can only make some hypothesis about it. Looking at Fig. 6b it is evident that most of the samples within the volcanic-geothermal field cluster around the following values: $\delta^{13}C \approx -21‰$ and $\delta^2H \approx -130‰$. Taking these values as the isotopic composition of CH_4 before oxidation, we obtain $\Delta H/\Delta C$ values comprised between 3.8 and 13.6 mostly overlapping the typical range of biogenic oxidation processes. Furthermore, the strongly positive values shown by some samples imply low values of the residual fraction of CH_4 (< 0.25).

The relationship between $\delta^{13}C$ values of CO_2 and CH_4 can be used to obtain useful information about the origin of these gas compounds (Whiticar et al., 1986). Assuming the attainment of an isotopic equilibrium between CH_4 and CO_2, equilibrium temperatures between the two gases can be computed according to Bottinga (1969) and Horita (2001). The estimation of the reservoir temperature through these geothermometers is outside the scope of this work. Nevertheless, most gases from VA and some thermal samples from IH and HH cover an estimated temperature interval between 270 and 500 °C indicating the possible achievement of isotopic equilibrium between CH_4 and CO_2. Among these, only for samples collected at Nisyros fumaroles Fiebig et al. (2004, 2007) demonstrated the attainment of equilibrium through the comparison with chemical geothermometers and temperatures measured in exploration wells. For all other samples, though indicating temperatures that are reasonable for geothermal systems, there is no proof for carbon isotope equilibration and the estimations may be likely only fortuitous. Instead all the samples plotting above the 700 °C isotherm are likely affected by secondary processes that isotopically fractionate CO_2 and CH_4. Such processes, as evidenced previously, are the CO_2 loss and the microbially-driven CH_4 oxidation. The former affects only the $\delta^{13}C$-CO_2 through either gas dissolution in water or precipitation as carbonate, whereas the latter tends toward more positive $\delta^{13}C$-CH_4 values and more negative $\delta^{13}C$-CO_2 values (Fig. 5b).

As shown in Fig. 7, the CH_4/C_2H_6 concentration ratios of the gas emissions vary by more than four orders of magnitude. On the contrary, the ratios between the main light hydrocarbons, i.e. C_2H_6, C_3H_8 and C_6H_6, vary only within two orders of magnitude. In this respect, the CO_2(CO)–CH_4 interaction that likely controls the CH_4 abundance in volcanic fluids does not seem to affect the higher hydrocarbons whose origin could be entirely related to thermal degradation of organic matter (Fiebig et al., 2009, 2015).

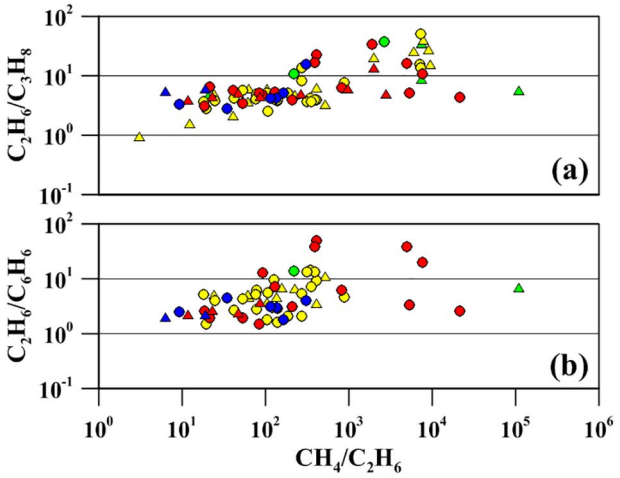

Fig. 7. a) CH_4/C_2H_6 vs. C_2H_6/C_3H_8 and b) CH_4/C_2H_6 vs. C_2H_6/C_6H_6 binary diagrams for the Hellenic gas discharges. Symbols as in Fig. 3.

CH_4 polymerization is accompanied by relatively small carbon isotope fractionations between C_{2+} *n*-alkanes and residual CH_4 (Sherwood Lollar et al., 2006; McCollom et al., 2010). This hypothesis should be supported by C-isotope data on C_{2+} alkane series' that unfortunately are not available for this study. Likewise, the residual CH_4 retains its primary carbon isotopic composition if the degree of polymerization is low. This, alternatively, might provide an explanation why there occurs no significant correlation between the ^{13}C composition of CH_4 and the magnitude of the Bernard ratio values for gases from VA (Fig. 6a), with $\delta^{13}C$-CH_4 being entirely controlled by $\delta^{13}C$-CO_2 and temperature.

5. Conclusions

Our results show that CH_4 from the Hellenic territory describes a wide range of both concentrations (from < 0.5 to 925,200 μmol/mol) and isotopic values ($\delta^{13}C$-CH_4 from −79.8 to +45.0‰; δ^2H-CH_4 from −311 to +301‰). Furthermore, the $CH_4/(C_2H_6 + C_3H_8)$ concentration ratio displays a broad range of values (1.5–93,200). Such a large variability in hydrocarbon concentration ratios and methane isotopic compositions is indicative for methane originating from different sources and for the importance of secondary, post genetic processes such as microbial oxidation. A schematic concluding description of the results combined with the variations of the geology, the heat flow values, and CO_2 and CH_4 concentrations along the Hellenic territory is proposed in the summary flow chart diagram (Fig. 8).

Taking into account the different lithological facies of the study area and the dominant gas species, it is noticeable that samples found on the western part of Greece (EH) display higher CH_4 and N_2 concentrations with respect to those found in the eastern part (IH, HH) where CO_2 is the prevailing gas. This can be explained by the sedimentary regime that characterises the EH, in which solid organic substances dominate, favouring the occurrence of hydrocarbon deposits. Moreover, the continuous changes in the relief and the mainly intrusive and metamorphic formations of both IH and HH contain few or no amounts of organic matter.

Biogenic methane was mainly found in the N_2-CH_4 and CH_4-dominated gases from EH. More specifically, gases collected in the Gavrovo-Tripolis zone show a dominating microbial origin. Gas samples of the Ionian and Pindos zones are produced by both microbial activity and thermal maturation of sedimentary organic matter. On the contrary

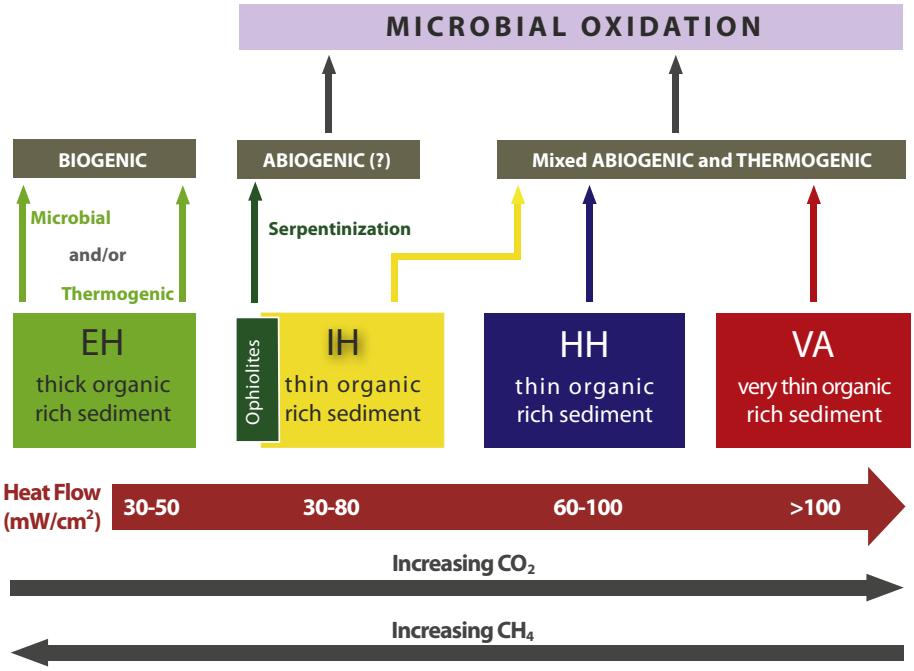

Fig. 8. A graphical description of the different possible origins of CH_4 including postgenetic processes. Connectors are emerging from the central boxes to the possible origins and the processes that are affecting its origin. The main boxes provide information about the thickness of the sedimentary sequences in the different geologic regions. Both variations of heat flow values and CO_2 and CH_4 concentrations along the regions are plotted on the lower part of the flow chat.

pure thermogenic samples are less represented in the sampled manifestations and are connected either to high geothermal gradients (samples 21 and 75) or to very thick sedimentary sequences in the Ionian (EH) and Aegean Sea (IH) (samples 104, 105 and 110 to 113).

Hydrocarbons contained in CO_2-rich thermal manifestations from HH (Rhodope massif) and IH (Pelagonian and Subpelagonian zones) are – regarding their isotopic composition – similar to those emitted from the crystalline or metamorphic rocks of the Precambrian shield (Sherwood Lollar et al., 2006). They, therefore, may be considered of abiogenic origin. However, for most of these samples, the measured values could also be explained by a biogenic origin modified by methane oxidation processes.

CO_2 dominated thermal gases from VA and N_2-CO_2-dominated thermal gases from IH show a relatively narrow range of $\delta^{13}C$-CH_4 values (−25 to −15‰) and a much larger range of $CH_4/(C_2H_6 + C_3H_8)$ concentration ratios (10 to 10,000) that show chemical and isotopic characteristics that are apparently consistent with an abiogenic origin for CH_4 with a minor contribution of a thermogenic source. For the geothermal system of Nisyros, which belongs to the VA, CH_4 is mostly originated from inorganic reactions in the hydrothermal reservoir while the light hydrocarbons have a prevailingly thermogenic origin (Fiebig et al., 2009).

Some of the N_2-rich gas manifestations of the IH collected in Pindos zone, seem to have a possible abiogenic origin for CH_4 as they are associated with the ophiolitic sequences of Othrys and Argolida. Finally, microbial oxidation processes have been evidenced for some of the CO_2-dominated gas discharges from the main thermal springs located in the Subpelagonian and Vardar-Axios zones (IH) and in the Rhodope massif (HH). Such processes lead to sometimes very strong isotopic fractionation of CH_4 reaching very positive $\delta^{13}C$ (+45.0‰) and $\delta^{2}H$ (+301‰) values.

Finally, we want to underscore that, although further studies are necessary to answer a number of questions that remained open such as the accurate origin of hydrocarbons, the important contribution of this paper is to show how hydrocarbons from all over Greece distribute in the Schoell and Bernard plots. Considering this, our study may be a starting point for those who want to investigate the geochemistry of fluids from a specific area included in this study and to examine in more detail their origin by applying new scientific approaches, such as those based on clumped isotopes.

Supplementary data to this article can be found online at https://doi.org/10.1016/j.chemgeo.2018.01.027.

Acknowledgments

We kindly acknowledge all the friends and colleagues that helped us either in the field or with precious information about the sampling sites. Among them we are indebted with Dr. Markos Xenakis and Dr. Konstantinos Athanasoulis of the IGME for their precious information about the location of many interesting sites all around the Hellenic territory. Also we would like to thank Francesco Capecchiacci (GC laboratory, UniFi), Mauro Martelli and Francesco Salerno (GC laboratory INGV-Pa), Ygor Oliveri and Aldo Sollami (MS laboratory INGV-Pa), Andrea Rizzo and Mariano Tantillo (Noble Gas laboratory INGV-Pa) for their kind and valuable support in the analyses and Silvia Eleonora Angileri and Stefano Dell'Aria for their useful help in drawing some of the figures. This work is part of the PhD thesis research of the first author (PhD in Earth and Marine Sciences – University of Palermo, 30th cycle and PhD in Applied Environmental Geology – National and Kapodistrian University of Athens). We are grateful for the insightful comments of Andri Stefánsson and an anonymous referee and of the editor Hailiang Dong that helped us to significantly improve the manuscript. We are also indebted to David Hilton, who managed as editor the first round of review of the manuscript. We were deeply touched by the notice of his death. Many of us knew him personally and we would like to express all our admiration for his human and scientific qualities.

References

Anders, B., Reischmann, T., Kostopoulos, D., 2006. The oldest rocks of Greece: first evidence for a Precambrian terrane within Pelagonian Zone. Geol. Mag. 143, 41–58.
Barnes, I., O'Neil, J.R., 1969. The relationship between fluids in some fresh alpine type ultramafics and possible modern serpentinization, western United States. Geol. Soc. Am. Bull. 80, 1947–1960.
Bernard, B.B., Brooks, J.M., Sackett, W.M., 1978. A Geochemical Model for Characterization of Hydrocarbon Gas Sources in Marine Sediments. Offshore Technology Conference, Houston, USA, pp. 435–438.
Berndt, M.E., Allen, D.E., Seyfried, W.E., 1996. Reduction of CO_2 during serpentinization of olivine at 300 °C and 500 bar. Geology 24, 351–354.
Bortolotti, V., Principi, G., 2005. Tethyan ophiolites and Pangea break-up. Island Arc 14, 442–470.
Bottinga, Y., 1969. Calculated fractionation factors for carbon and hydrogen isotope

exchange in the system calcite-carbon dioxide-graphite-methane-hydrogen-water vapor. Geochim. Cosmochim. Acta 33, 49–64.
Bradley, A.S., Summons, R.E., 2010. Multiple origins of methane at the Lost City hydrothermal field. Earth Planet. Sci. Lett. 297, 34–41.
Bruni, J., Canepa, M., Cipolli, F., Marini, L., Ottonello, G., Vetuschi Zuccolini, M., et al., 2002. Irreversible water-rock mass transfer accompanying the generation of the neutral, Mg-HCO_3 and high-pH, Ca-OH spring waters of the Genova province, Italy. Appl. Geochem. 17, 455–474.
Burke, R.A., Barber, T., Sackett, W., 1988. Methane flux and stable H and C isotope composition of the sedimentary methane from the Florida Everglades. Glob. Biogeochem. Cycles 2, 329–340.
Burke, R.A., Martens, C.S., Sackettl, W., 1988. Seasonal variations of D/H and $^{13}C/^{12}C$ ratios of microbial methane in surface sediments. Nature 332, 829–831.
Burton, P., Xu, Y., Qin, C., Tselentis, G., Sokos, E., 2004. A catalogue of seismicity in Greece and the adjacent areas of the twentieth century. Tectonophysics 390, 117–127.
Cadieux, S.B., White, J.R., Sauer, P.E., Peng, Y., Goldman, A.E., Pratt, L.M., 2016. Large fractionations of C and H isotopes related to methane oxidation in Arctic lakes. Geochim. Cosmochim. Acta 187, 141–155.
Capaccioni, B., Martini, M., Mangani, F., Giannini, L., Nappi, G., Prati, F., 1993. Light hydrocarbons in gas-emissions from volcanic areas and geothermal fields. Geochem. J. 27, 7–17.
Capaccioni, B., Taran, Y., Tassi, F., Vaselli, O., Mangani, G., Macias, J.L., 2004. Source conditions and degradation processes of light hydrocarbons in volcanic gases: an example from El Chichon volcano (Chiapas State, Mexico). Chem. Geol. 206, 81–96.
Capasso, G., Inguaggiato, S., 1998. A simple method for the determination of dissolved gases in natural waters. An application to thermal waters from Vulcano Island. Appl. Geochem. 13, 631–642.
Cavazza, W., Roure, F., Spakman, W., Stampfli, G.M., Ziegler, P.A., 2014. The TRANSMED Atlas – The Mediterranean Region from Crust to Mantle Geological and Geophysical Framework of the Mediterranean and the Surrounding Areas. Springer, Verlag Berlin, Heidelberg, New York, NY.
Chanton, J.P., Chasar, L.C., Glaser, P., Siegel, D., 2005. Carbon and hydrogen isotopic effects in microbial methane from terrestrial environments. In: Flanagan, L.B., Ehleringer, J.R., Pataki, D.E. (Eds.), Stable Isotopes and Biosphere-Atmosphere Interactions. Physiol. Ecol. Ser., vol. 6. Elsevier, New York, pp. 85–105.
Chiodini, G., 1994. Temperature, pressure and redox conditions governing the composition of the cold CO_2 gases discharged in the volcanic area of North Latium (Central Italy). Appl. Geochem. 9, 287–295.
Ciais, P., Sabine, C., Bala, G., Bopp, L., Brovkin, V., Canadell, J., Chabra, A., De Fries, R., Galloway, J., Heimann, M., Jones, C., Le Quéré, C., Myneni, R.B., Piao, S., Thornton, P., 2013. Carbon and other biogeochemical cycles. In: Stocker, T.F. (Ed.), Climate Change 2013: The Physical Science Basis. Contribution of Working Group I to the Fifth Assessment Report of IPCC. Cambridge University Press, Cambridge.
Coleman, D.D., Risatti, J.B., Schoell, M., 1981. Fractionation of carbon and hydrogen isotopes by methane-oxidizing bacteria. Geochim. Cosmochim. Acta 45, 1033–1037.
D'Alessandro, W., Brusca, L., Kyriakopoulos, K., Bellomo, S., Calabrese, S., 2014. A geochemical traverse along the "Sperchios Basin — Evoikos Gulf" Graben (Central Greece): origin and evolution of the emitted fluids. Mar. Pet. Geol. 55, 295–308. http://dx.doi.org/10.1016/j.marpetgeo.2013.12.011.
D'Alessandro, W., Daskalopoulou, K., Calabrese, S., Bellomo, S., 2017. Water chemistry and abiogenic methane content of a hyperalkaline spring related to serpentinization in the Argolida ophiolite (Ermioni, Greece). Mar. Pet. Geol. http://dx.doi.org/10.1016/j.marpetgeo.2017.01.028.
D'Alessandro, W., Kyriakopoulos, K., 2013. Preliminary gas hazard evaluation in Greece. Nat. Hazards 69, 1987–2004.
Darling, W.G., 1998. Hydrothermal hydrocarbons gases: 1. Genesis and geothermometry. Appl. Geochem. 13, 815–824.
Dercourt, J., 1972. The Canadian cordillera, the Hellenides and the sea floor spreading theory. Can. J. Earth Sci. 9, 709–743.
Dimitrakopoulos, R., Muehlenbachs, K., 1987. Biodegradation of petroleum as a source of ^{13}C enriched carbon dioxide in the formation of carbonate cements. Chem. Geol. 65, 283–291.
Etiope, G., 2009. A Global Dataset of Onshore Gas and Oil Seeps: A New Tool for Hydrocarbon Exploration. Oil and Gas Business. http://ogbus.ru/eng/authors/Etiope/Etiope_1.pdf (accessed 07/07/2017).
Etiope, G., 2015. Natural Gas Seepage. The Earth's Hydrocarbon Degassing. Springer International Publishing Switzerland, pp. 119. e-book. Ch 7.1.5. https://doi.org/10.1007/978-3-319-14601-0.
Etiope, G., Sherwood Lollar, B., 2013. Abiotic methane on Earth. Rev. Geophys. 51, 276–299. http://dx.doi.org/10.1002/rog.20011.
Etiope, G., Schoell, M., 2014. Abiotic gas: atypical but not rare. Elements 10, 291–296.
Etiope, G., Ionescu, A., 2015. Low-temperature catalytic CO_2 hydrogenation with geological quantities of ruthenium: a possible abiotic CH_4 source in chromite-rich serpentinized rocks. Geofluids 15, 438–452.
Etiope, G., Papatheodorou, G., Christodoulou, D., Ferentinos, G., Sokos, E., Favali, P., 2006. Methane and hydrogen sulfide seepage in the NW Peloponnesus petroliferous basin (Greece): origin and geohazard. AAPG Bull. 90, 701–713.
Etiope, G., Caracausi, A., Favara, R., Italiano, F., Baciu, C., 2009. Methane emission from the mud volcanoes of Sicily (Italy). J. Geophys. Res. Lett. 29 (8), 1215.
Etiope, G., Christodoulou, D., Kordella, S., Marinaro, G., Papatheodorou, G., 2013a. Offshore and onshore seepage of thermogenic gas at Katakolo Bay (Western Greece). Chem. Geol. 339, 115–126.
Etiope, G., Tsikouras, B., Kordella, S., Ifandi, E., Christodoulou, D., Papatheodorou, G., 2013b. Methane flux and origin in the Othrys ophiolite hyperalkaline springs, Greece. Chem. Geol. 347, 161–174.
Ferrière, J., Baumgartner, P.O., Chanier, F., 2016. The Maliac Ocean: the origin of Tethyan Hellenic ophiolites. Int. J. Earth Sci. 105, 1941–1963. http://dx.doi.org/10.1007/s00531-016-1303-6.
Fiebig, J., Chiodini, G., Caliro, S., Rizzo, A., Spandenberg, J., Hunziker, J.C., 2004. Chemical and isotopic equilibrium between CO_2 and CH_4 in fumarolic gas discharges: generation of CH_4 in arc magmatic-hydrothermal systems. Geochim. Cosmochim. Acta 68, 2321–2334.
Fiebig, J., Hofmann, S., Tassi, F., D'Alessandro, W., Vaselli, O., Woodland, A.B., 2015. Isotopic patterns of hydrothermal hydrocarbons emitted from Mediterranean volcanoes. Chem. Geol. 396, 152–163. http://dx.doi.org/10.1016/j.chemgeo.2014.12.030.
Fiebig, J., Tassi, F., D'Alessandro, W., Vaselli, O., Woodland, A., 2013. Carbon-bearing gas geothermometers for volcanic-hydrothermal systems. Chem. Geol. 351, 66–75.
Fiebig, J., Woodland, A., D'Alessandro, W., Puttmann, W., 2009. Excess methane in continental hydrothermal emissions is abiogenic. Geology 37, 495–498.
Fiebig, J., Woodland, A.B., Spangenberg, J., Oschmann, W., 2007. Natural evidence for rapid abiogenic hydrothermal generation of CH_4. Geochim. Cosmochim. Acta 71, 3028–3039.
Fischer, F., Tropsch, H., 1923. The preparation of synthetic oil mixtures (synthol) from carbon monoxide and hydrogen. Brennst. Chem. 4, 276–285.
Fischer, F., Tropsch, H., 1926. Über die direkte Synthese von Eerdöl-kohlenwasserstoffen bei gewöhnlichtem Druck. Ber. Dtsch. Chem. Ges. 59, 830–831.
Formolo, M., 2010. The microbial production of methane and other volatile hydrocarbons. In: Kenneth, N. (Ed.), Timmis Handbook of Hydrocarbon and Lipid Microbiology. Springer, New York, pp. 113–126.
Foustoukos, D.I., Seyfried, W.E., 2004. Hydrocarbons in hydrothermal vent fluids: the role of chromium-bearing catalysts. Science 304, 1002–1004.
Fytikas, M., Innocenti, F., Kolios, N., Manetti, P., Mazzuoli, R., 1986. The Plio-Quaternary volcanism of the Saronikos area (western part of the active Aegean volcanic arc). Ann. Géol. Pays Hellén. 33, 23–45.
Fytikas, M., Kolios, N., 1979. Preliminary heat flow map of Greece. In: Cermak, V., Rybach, L. (Eds.), Terrestrial Heat Flow in Europe. Springer-Verlag, Berlin Heidelberg New York, pp. 197–205.
Giggenbach, W.F., 1980. Geothermal gas equilibria. Geochim. Cosmochim. Acta 44, 2021–2032.
Giggenbach, W.F., 1987. Redox processes governing the chemistry of fumarolic gas discharges from White Island, New Zealand. Appl. Geochem. 2, 143–161.
Giggenbach, W.F., 1996. Chemical composition of volcanic gases. In: Scarpa, R., Tilling, R.I. (Eds.), Monitoring and Mitigation of Volcano Hazards. Springer, pp. 221–256.
Giggenbach, W.F., Gougel, R.L., 1989. Method for the collection and analysis of geothermal and volcanic water and gas samples. NZ-DSIR Report CD 2387, 53.
Grassa, F., Capasso, G., Oliveri, Y., Sollami, A., Carreira, P., Rosário Carvalho, M., Marques, J.M., Nunes, J.C., 2010. Nitrogen isotopes determination in natural gas: analytical method and first results on magmatic, hydrothermal and soil gas samples. Isot. Environ. Health Stud. 46, 141–155.
Grigoriadis, V., Tziavos, I., Tsokas, G., Stampolidis, A., 2016. Gravity data inversion for Moho depth modeling in the Hellenic area. Pure Appl. Geophys. 173, 1223–1241. 2015 Springer Basel DOI. https://doi.org/10.1007/s00024-015-1174-y.
Guliyev, I.S., Feizullayev, A.A., 1997. All about mud volcanoes. Baku Pub. House, NAFTA-Press (120 pp.).
Gunter, B.D., 1978. C1–C4 hydrocarbons in geothermal gases. Geochim. Cosmochim. Acta 42, 137–139.
Hinrichs, K.U., Hayes, J.M., Bach, W., Spivack, A.J., Hmelo, L.R., Holm, N.G., Johnson, C.G., Sylva, S.P., 2006. Biological formation of ethane and propane in the deep marine subsurface. Proc. Natl. Acad. Sci. 103 (40), 14684–14689. http://dx.doi.org/10.1073/pnas.0606535103.
Holloway, J.R., 1984. Graphite-CH_4-H_2O-CO_2 equilibria at low-grade metamorphic conditions. Geology 12, 455–458.
Horita, J., 2001. Carbon isotope exchange in the system CO_2-CH_4 at elevated temperatures. Geochim. Cosmochim. Acta 65, 1907–1919.
Horita, J., Berndt, M.E., 1999. Abiogenic formation and isotopic fractionation under hydrothermal conditions. Science 285, 1055–1057.
Hornibrook, E.R.C., Longstaffe, F.J., Fyfe, W.S., 1997. Spatial distribution of microbial methane production pathways in temperate zone wetland soils: stable carbon and hydrogen isotope evidence. Geochim. Cosmochim. Acta 61 (4), 745–753.
Hunt, J.M., 1996. Petroleum Geochemistry and Geology, 2nd ed. W.H. Freeman Co., New York (743 pp.).
Jenden, P.D., Hilton, D.R., Kaplan, I.R., Craig, H., 1993. Abiogenic hydrocarbons and mantle helium in oil and gas fields. In: Howell, D.G. (Ed.), The Future of Energy Gases: US Geol. Surv. Profes. Paper. vol. 1570. pp. 31–56.
Kamberis, E., Rigakis, N., Tsaila-Monopolis, S., Ioakim, C., Sotiropoulos, S., 2000. Shallow biogenic gas-accumulations in late Cenozoic sands of Katakolon Peninsula, western Greece. Geol. Soc. Greece, Spec. Publ. 9, 121–138.
Kanellopoulos, C., 2012. Distribution, lithotypes and mineralogical study of newly formed thermogenic travertines in Northern Euboea and Eastern Central Greece. Cent. Eur. J. Geosci. 4 (4), 545–560. http://dx.doi.org/10.2478/s13533-012-0105-z.
Kanellopoulos, C., Mitropoulos, P., Valsami-Jones, E., Voudouris, P., 2017. A new terrestrial active mineralizing hydrothermal system associated with ore-bearing travertines in Greece (northern Euboea Island and Sperchios area). J. Geochem. Explor. 179, 9–24.
Kietäväinen, R., Purmako, L., 2015. The origin, source, and cycling of methane in deep crystalline rock biosphere. Front. Microbiol. 6, 725.
Kinnaman, F.S., Valentine, D.L., Tyler, S.C., 2007. Carbon and hydrogen isotope fractionation associated with the aerobic microbial oxidation of methane, ethane, propane and butane. Geochim. Cosmochim. Acta 71, 271–283.
Kiyosu, Y., Imaizumi, S., 1996. Carbon and hydrogen isotope fractionation during oxidation of methane by metal oxides at temperatures from 400° to 530 °C. Chem. Geol. 133, 279–287.
Klusman, R.W., Jakel, M.E., 1998. Natural microseepage of methane to the atmosphere from the Denver-Julesburg basin, Colorado, USA. J. Geophys. Res. 103D, 28,042–28,045.
Konn, C., Charlou, J.L., Holm, N.G., Mousis, O., 2015. The production of methane, hydrogen, and organic compounds in ultramafic- hosted hydrothermal vents of the Mid-Atlantic Ridge. Astrobiology 15 (5), 381–399.

Kvenvolden, K.A., 1993. Gas hydrates—geological perspective and global change. Rev. Geophys. 31, 173–187.
Machel, H.G., Krouse, H.R., Sassen, R., 1995. Products and distinguishing criteria of bacterial and thermochemical sulphate reduction. Appl. Geochem. 10, 373–389.
Mango, F.D., 2000. The origin of light hydrocarbons. Geochim. Cosmochim. Acta 64, 1265–1277.
Marini, L., Fiebig, J., 2005. Fluid geochemistry of the magmatic-hydrothermal system of Nisyros (Greece). Memoires Geol. (Lausanne) 44, 121–163.
McCollom, T.M., 2013. Laboratory simulations of abiotic hydrocarbon formation in Earth's deep subsurface. Rev. Mineral. Geochem. 75, 467–494.
McCollom, T.M., Seewald, J.S., 2007. Abiotic synthesis of organic compounds in deep-sea hydrothermal environments. Chem. Rev. 107, 382–401.
McCollom, T.M., Sherwood Lollar, B., Lacrampe-Couloume, G., Seewald, J.S., 2010. The influence of carbon source on abiotic organic synthesis and carbon isotope fractionation under hydrothermal conditions. Geochim. Cosmochim. Acta 74, 2717–2740.
Milkov, A.V., 2000. Worldwide distribution of submarine mud volcanoes and associated gas hydrates. Mar. Geol. 167, 29–42.
Miller, H.M., Mayhew, L.E., Ellison, E.T., Kelemen, P., Kubo, M., Templeton, A.S., 2017. Low temperature hydrogen production during experimental hydration of partially-serpentinized dunite. Geochim. Cosmochim. Acta 209, 161–183.
Minissale, A., 2004. Origin, transport and discharge of CO_2 in central Italy. Earth Sci. Rev. 66, 89–141.
Mörner, N.A., Etiope, G., 2002. Carbon degassing from the lithosphere. Glob. Planet. Chang. 33, 185–203.
Mountrakis, D.M., 1985. Geologia tis Elladas. University Studio Press, Thessaloniki, pp. 207 (in Greek).
Mountrakis, D.M., 1986. The Pelagonian zone in Greece: a Polyphase-deformed fragment of the Cimmerian continent and its role in the geotectonic evolution of the Eastern Mediterranean. J. Geophys. 94, 335–347.
Mountrakis, D.M., 2010. Geologia kai Geotektoniki Exelixi tis Elladas. University Studio Press, Thessaloniki, pp. 374 (in Greek).
Murrell, C.J., Jetten, M.S.M., 2009. The microbial methane cycle. Environ. Microbiol. Rep. 1, 279–284.
Palacas, J.G., Monopolis, D., Nicolaou, C.A., Anders, D.E., 1986. Geochemical correlation of surface and subsurface oils, western Greece. Org. Geochem. 10, 417–423.
Pallasser, R.J., 2000. Recognising biodegradation in gas/oil accumulations through the δ^{13} compositions of gas components. Org. Geochem. 31, 1363–1373.
Paonita, A., Caracausi, A., Iacono-Marziano, G., Martelli, M., Rizzo, A., 2012. Geochemical evidence for mixing between fluids exsolved at different depths in the magmatic system of Mt Etna (Italy). Geochim. Cosmochim. Acta 84, 380–394.
Papanikolaou, D., 2009. Timing of tectonic emplacement of the ophiolites and terrane paleogeography in the Hellenides. Lithos 108, 262–280.
Pe-Piper, G., Piper, D.J.W., 2002. The igneous rocks of Greece, The anatomy of an orogen. In: Beiträge Zur Regionalen Geologie der Erde. vol. 30 Gebrüder Bornträger, Berlin - Stuttgart.
Prinzhofer, A.A., Battani, A., 2003. Gas isotopes tracing: an important tool for hydrocarbon exploration. Oil Gas Sci. Technol. 58, 229–311.
Proskurowski, G., Lilley, M., Seewald, J.S., Fruh-Green, G.I., Olson, E.J., Sylva, S.P., Kelley, D.S., 2008. Abiogenic hydrocarbon production at Lost City hydrothermal field. Science 319, 604–607.
Proskurowski, G., Lilley, M.D., Kelley, D.S., Olson, E.J., 2006. Low temperature volatile production at the Lost City hydrothermal field, evidence from a hydrogen stable isotope geothermometer. Chem. Geol. 229, 331–343.
Quingley, T.M., MacKenzie, A.S., 1988. The temperatures of oil and gas formation in the sub-surface. Nature 333, 549–552.
Reischmann, T., Kostopoulos, D., 2007. Terrane accretion in the internal Hellenides. Geophys. Res. Abstr. 9, 05337.
Rigakis, N., Roussos, N., Kamberis, E., Proedrou, P., 2001. Hydrocarbon gas accumulations in Greece and their origin. Bull. Geol. Soc. Greece 34 (3), 1265–1273.
Rizzo, A.L., Barberi, F., Carapezza, M.L., Di Piazza, A., Francalanci, L., Sortino, F., D'Alessandro, W., 2015. New mafic magma refilling a quiescent volcano: evidence from He-Ne-Ar isotopes during the 2011–2012 unrest at Santorini, Greece. Geochem. Geophys. Geosyst. 16. http://dx.doi.org/10.1002/2014GC005653.
Roberts, G.P., Koukouvelas, L., 1996. Structural and seismological segmentation of the Gulf of Corinth fault system: implications for models of fault growth. Ann. Geophys. 39 (3), 619–646.
Robertson, A.H.F., 2004. Development of concepts concerning the genesis and emplacement of Tethyan ophiolites in the Eastern Mediterranean and Oman regions. Earth-Sci. Rev. 66, 331–387.
Robertson, A.H.F., 2012. Late Palaeozoic–Cenozoic tectonic development of Greece and Albania in the context of alternative reconstructions of Tethys in the Eastern Mediterranean region. Int. Geol. Rev. 54, 373–454.
Robertson, A.H.F., Dixon, J.F., 1984. Introduction: aspects ofthe geological evolution ofthe Eastem Mediterranean. In: Dixon, J.E., Robertson, A.H.F. (Eds.), The Geological Evolution of the Eastern Mediterranean. Geol. Soc. London Spec. Publ. Vol. 17. pp. 1–74.
Sano, Y., Marty, B., 1995. Origin of carbon in fumarolic gas from island arcs. Chem. Geol. 119, 265–274.
Schoell, M., 1980. The hydrogen and carbon isotopic composition of methane from natural gases of various origins. Geochim. Cosmochim. Acta 44, 649–661.
Schoell, M., 1988. Multiple origins of methane in the Earth. Chem. Geol. 71, 1–10.
Seewald, J.S., 2001. Aqueous geochemistry of low molecular weight hydrocarbons at elevated temperatures and pressures. Constraints from mineral buffered laboratory experiments. Geochim. Cosmochim. Acta 65, 1641–1664.
Sharp, C.E., Smirnova, A.V., Graham, J.M., Stott, M.B., Khadka, R., Moore, T.R., Grasby, S.E., Strack, M., Dunfield, P.F., 2014. Distribution and diversity of Verrucomicrobia methanotrophs in geothermal and acidic environments. Environ. Microbiol. 16, 1867–1878.
Sherwood Lollar, B., Lacrampe-Couloume, G., Slater, G.F., Ward, J.A., Moser, D.P., Gihring, T.M., Lin, L.H., Onstott, T.C., 2006. Unravelling abiogenic and biogenic sources of methane in the Earth's deep subsurface. Chem. Geol. 226, 328–339.
Smith, A.G., Moores, E.M., 1974. Hellenides. Geol. Soc. Lond. Spec. Publ. 4, 159–185.
Snyder, G., Poreda, R.J., Fehn, U., Hunt, A., 2003. Sources of nitrogen and methane in Central American geothermal settings: noble gas and ^{129}I evidence for crustal and magmatic volatile components. Geochem. Geophys. Geosyst. 4. http://dx.doi.org/10.1029/2002GC000363.
Snyder, G., Poreda, R.J., Hunt, A., Fehn, U., 2001. Regional variations in volatile composition: isotopic evidence for carbonate recycling in the Central American volcanic arc. Geochem. Geophys. Geosyst. 2. http://dx.doi.org/10.1029/2001GC 000163.
Stampfli, G., Vavassis, I., De Bono, A., Rosselet, F., Matti, B., Bellini, M., 2003. Remnants of the Paleotethys oceanic suture-zone in the western Tethyan area. Boll. Soc. Geol. Ital., Spec. 2, 1–23.
Stefánsson, A., Lemke, K.H., Bènèzeth, P., Schott, J., 2017. Magnesium bicarbonate and carbonate interactions in aqueous solutions: an infrared spectroscopic and quantum chemical study. Geochim. Cosmochim. Acta 198, 271–284.
Stefánsson, A., Sveinbjörnsdòttir, A.E., Heinemeier, J., Arnòrsson, S., Kjartansdòttir, R., Kristmannsdòttir, H., 2016. Mantle CO_2 degassing through the Icelandic crust: evidence from carbon isotopes in groundwater. Geochim. Cosmochim. Acta 191, 300–319.
Stolper, D.A., Lawson, M., Davis, C.L., Ferreira, A.A., Santos Neto, E.V., Ellis, G.S., Lewan, M.D., Martini, A.M., Tang, Y., Schoell, M., Sessions, A.L., Eiler, J.M., 2014. Gas formation. Formation temperatures of thermogenic and biogenic methane. Science 344, 1500–1503.
Takai, K., Nakamura, K., Toki, T., Tsunogai, U., Miyazaki, M., Miyazaki, J., Hirayama, H., Nakagawa, S., Nunoura, T., Horikoshi, K., 2008. Cell proliferation at 122 °C and isotopically heavy CH_4 production by a hyperthermophilic methanogen under high pressure cultivation. Proc. Natl. Acad. Sci. 105, 10949–10954.
Taran, Y., Giggenbach, W., 2003. Geochemistry of light hydrocarbons in subduction-related volcanic and hydrothermal fluids. Society of Economic Geologists Special Publication 10 (6), 61–74.
Tassi, F., 2004. Fluidi in ambiente vulcanico: Evoluzione temporale dei parametri composizionali e distribuzione degli idrocarburi leggeri in fase gassosa (in Italian), Ph.D. thesis. Univ. of Florence, Florence, Italy, pp. 292.
Tassi, F., Fiebig, J., Vaselli, O., Nocentini, M., 2012. Origins of methane discharging from volcanic-hydrothermal, geothermal and cold emissions in Italy. Chem. Geol. 310–311, 36–48.
Tassi, F., Martinez, C., Vaselli, O., Capaccioni, B., Viramonte, J., 2005a. The light hydrocarbons as new geoindicators of equilibrium temperatures and redox conditions of geothermal fields: evidence from El Tatio (northern Chile). Appl. Geochem. 20, 2049–2062.
Tassi, F., Vaselli, O., Capaccioni, B., Giolito, C., Duarte, E., Fernandez, E., Minissale, A., Magro, G., 2005b. The hydrothermal-volcanic system of Rincon de la Vieja volcano (Costa Rica): a combined (inorganic and organic) geochemical approach to understanding the origin of the fluid discharges and its possible application to volcanic surveillance. J. Volcanol. Geotherm. Res. 148, 315–333.
Tilley, B., Muehlenbachs, K., 2013. Isotope reversals and universal stages and trends of gas maturation in sealed, self-contained petroleum systems. Chem. Geol. 339 (2013), 194–204.
van Hinsbergen, D.J.J., Hafkenscheid, E., Spakman, W., Meulenkamp, J.E., Wortel, M.J.R., 2005. Nappe stacking resulting from subduction of oceanic and continental lithosphere below Greece. Geology 33, 325–328.
Vaselli, O., Tassi, F., Montegrossi, G., Capaccioni, B., Giannini, L., 2006. Sampling and analysis of volcanic gases. Acta Vulcanol. 18, 65–76.
Wang, D.T., Gruen, D.S., Lollar, B.S., Hinrichs, K.U., Stewart, L.C., Holden, J.F., Hristov, A.N., Pohlman, J.W., Morrill, P.L., Könneke, M., Delwiche, K.B., Reeves, E.P., Sutcliffe, C.N., Ritter, D.J., Seewald, J.S., McIntosh, J.C., Hemond, H.F., Kubo, M.D., Cardace, D., Hoehler, T.M., Ono, S., 2015. Methane cycling. Nonequilibrium clumped isotope signals in microbial methane. Science 348 (6233), 428–431.
Welhan, J.A., 1988. Origins of methane in hydrothermal systems. Chem. Geol. 71, 183–198.
Welhan, J.A., Craig, H., 1983. Methane, hydrogen and helium in hydrothermal fluids of 21 °N on the East Pacific Rise. In: Rona, P.A., Boström, K., Laubier, L., Smith Jr.K.L. (Eds.), Hydrothermal Processes at Seafloor Spreading Centers. Plenum, New York, N.Y., pp. 391–409.
Whiticar, M.J., 1999a. Stable isotope geochemistry of coals, humic kerogen and related natural gases. Int. J. Coal Geol. 32, 191–215.
Whiticar, M.J., 1999b. Carbon and hydrogen isotope systematics of bacterial formation and oxidation of methane. Chem. Geol. 161, 291–314.
Whiticar, M.J., Faber, E., Schoell, M., 1986. Biogenic methane formation in marine and freshwater environments: CO_2 reduction vs. acetate fermentation - isotopic evidence. Geochim. Cosmochim. Acta 50, 693–709.
Whiticar, M.J., Suess, E., 1990. Hydrothermal hydrocarbon gases in the sediments of the King-George Basin, Bransfield Strait, Antarctica. Appl. Geochem. 5, 135–147.
Winkel, L.H.E., Casentini, B., Bardelli, F., Voegelin, A., Nikolaidis, N.P., Charlet, L., 2013. Speciation of arsenic in Greek travertine: co-precipitation of arsenate with calcite. Geochim. Cosmochim. Acta 106, 99–110.
Worden, R.H., Smalley, P.C., 1996. H_2S-producing reactions in deep carbonate gas reservoirs: Khuff Formation, Abu Dhabi. Chem. Geol. 133, 157–171.